Politics-driven Market Access and Its Cost: Evidence from China's Grand Canal*

Ying Bai† Xiaoyu Bian‡ Ruixue Jia§

September 2026

Abstract

Transportation networks often radiate from national capitals, reflecting political priorities as much as economic logic. How costly is infrastructure built for politics rather than markets? We study China's Grand Canal: when the Mongols moved the capital from the central plain to Beijing, the canal followed, bypassing the economic core it once served. Using a grid-year panel spanning five dynasties (8th–19th centuries), we show the route best suited to reach the capital predicts the canal's actual path. This redesign reshaped market access and, through it, population. Counterfactual analysis shows the canal raised population by 2.5–6.1%, but its politically motivated redesign cost 1.1–2.2%.

Keywords: Politics-driven Infrastructure; Market Access; Misallocation
JEL Codes: O18, R12, N75, N45

*We thank Treb Allen, Ben Faber, Noam Yuchtman and seminar/conference participants at Workshop on Trade and Economic Geography at CUHK, Workshop on the New Economic History of China at University of Melbourne, Macro Workshop of CUHK-Tsinghua Joint Research Center for Chinese Economy, and HKU. Ying Bai acknowledges financial support from the University Grants Committee/Research Grants Council of the Hong Kong Special Administrative Region, China (project no. AoE/B-704/22-R). All remaining errors are ours.

†University of Hong Kong. yingbai@hku.hk
‡Nankai University. xiaoyubianhk@gmail.com
§UCSD, CEPR and NBER; visiting professor, University of Hong Kong. rxjia@ucsd.edu

1 Introduction

In many countries, the national capital functions as a central hub for transportation networks, shaped by its political and administrative significance. These networks often radiate outward from the capital, linking it to key regions of the nation and solidifying its role as a core of governance, commerce, and connectivity. As shown in Figure 1, Beijing's extensive rail and road networks, including its high-speed rail system, create vital links to all corners of China, reinforcing the capital's centrality in national logistics. Similarly, Delhi serves as the anchor of India's transportation system, with its metro network seamlessly integrating the National Capital Region (NCR) and a convergence of national highways ensuring connectivity. Paris exemplifies France's hub-and-spoke transportation model, where the TGV high-speed rail and radial road systems center on the capital to facilitate efficient movement. Moscow mirrors this pattern as Russia's transportation heart, with radial railways and the Trans-Siberian Railway extending from the capital to connect vast, remote regions to the political core. These examples illustrate that a national capital is not merely one node among many in a transportation network: it is the anchor point around which the network's entire spatial structure, and hence the market access of the nation, is organized.

This raises a question that goes beyond how politics affects city size and local development, a relationship already studied by existing literature (e.g., De Long and Shleifer, 1993; Ades and Glaeser, 1995; Campante and Do, 2014; Campante, Do and Guimaraes, 2019). Market access is inherently a general-equilibrium object: a location's access to markets depends on the whole network connecting it, so relocating a single anchor node can reshape market access across an entire territory. A large literature has documented that infrastructure raises market access and economic activity, pioneered by Donaldson and Hornbeck (2016).[1] Yet this literature speaks mostly to infrastructure sited by economic logic and documents its benefits. When a network's anchor point is instead set by political priorities, it remains an open question whether the resulting infrastructure creates net economic value in the aggregate, and, even if it does, whether serving the political anchor misallocates resources. The core empirical challenge is identification: national capitals rarely relocate, so there is usually no variation that separates a political motive for infrastructure from an economic one.

China's Grand Canal is well suited to filling this gap. The canal originated in local waterways connected into a single network by the early 7th century, and as long as the capital stayed in or

[1] A growing literature estimates the impacts of market access, such as Duranton, Morrow and Turner (2014), Alder (2025), Yang (2018), Jaworski and Kitchens (2019), Heblich, Redding and Sturm (2020), Hornbeck and Rotemberg (2024), and Balboni (2025).

near the central plain, moving between Xi'an, Luoyang, and Kaifeng under the Sui, Tang, and Song, this network needed no dramatic redesign. That changed in 1271, when the Mongol-founded Yuan dynasty reunified China and moved the capital far to the north, to Beijing, where it would remain through the Ming and Qing, forcing a wholesale rebuild that bypassed the central plain for a direct Beijing-Hangzhou route (Figure 2). Because the canal's purpose was explicitly to move troops, tribute grain, and officials to and from whichever city was capital, its history allows us to test whether the optimal route to connect to the capital predicts where the canal was built. This lets us trace not only whether the canal followed the capital, but how far the consequences of that political redesign reached: how it reshaped market access, and the population it supported, across the country.

We bring this history into a 1-degree $\times$ 1-degree grid-year panel spanning the Tang, Song, Yuan, Ming, and Qing dynasties (8th–19th centuries). Combining population census data for 741, 980, 1080, 1102, 1290, 1393, 1580, 1776, and 1820 with rich information on the transportation networks, including natural rivers, canals, and land routes, we construct a balanced panel of 361 grids over these nine sample periods. By measuring how costly each route type was to travel, drawing on historical research, we compute the minimum-cost route between every pair of grids in every sample period and, following Donaldson and Hornbeck (2016), construct a market access measure for each grid: the population of every other grid, discounted by how costly that grid is to reach. We also assemble a rich set of grid-level geographic and agricultural characteristics.

Using this panel, we begin with a standard fixed-effects specification that controls for grid and year fixed effects. We further control for a rich set of geographic and agricultural characteristics, allowing their effects to vary over time. To strengthen identification, we complement this design with event-study analyses and placebo tests. Together, these approaches establish three main results.

First, the Grand Canal follows the capital. For each dynasty we compute the route that would minimize the cost of connecting the national capital to the military frontier in the north and the economic core in the south, a route dictated by geography and by where the capital happened to be, with no reference to realized trade. This "optimal route to the capital" strongly predicts the canal's actual path: a 1-kilometer increase in the optimal route raises the actual waterway by approximately 0.87 kilometers. Our strategy is in the spirit of Faber (2014), who instrument for China's National Trunk Highway System using the hypothetical least-cost network connecting targeted cities. Our long panel also allows us to conduct placebo tests: the route optimal for reaching the Song capital predicts the actual waterway well before 1271 but loses its predictive power afterward, while the route optimal for reaching the Yuan capital shows the mirror-image pattern, gaining predictive

power only from 1271 onward. Market access built from this politically optimal network (even when holding population fixed) is, in turn, strongly correlated with market access built from the actual transportation network, confirming that it captures the consequences of a political decision rather than an economic one.

Second, this capital-induced market access raises local population density. We find that a 1% increase in market access raises population density by about 0.14%. The magnitude is similar with an Instrumental Variable (IV) approach, using the optimal-route market access as an instrument for actual market access. Our IV estimates hold when we restrict this market access to more distant grids, which mitigates the exclusion restriction concern that the optimal route may capture direct, place-based state investment, such as garrisons, courier stations, rather than market access. Moreover, when we isolate the sharp negative change in market access caused by the Song-Yuan canal redesign and trace out its period-by-period effect on population density, the impact shows no pre-trend before 1102 and turns sharply and permanently negative by 1290.

Third, capital-induced market access carries both aggregate benefits and real distortion. Embedding our estimates in a spatial equilibrium model (Donaldson and Hornbeck, 2016), we run two counterfactuals. Removing the Grand Canal from the network altogether would have lowered aggregate population by 2.5–6.1%. But the specific route also mattered: had the Ming and Qing dynasties kept the earlier canal through the central plain instead of the direct Beijing-Hangzhou route, aggregate population would have been 1.1–2.2% higher.[2] These counterfactual estimates are smaller than the corresponding reduced-form projections that omit general-equilibrium forces, but they remain economically sizable. The Grand Canal was therefore not wasteful in the aggregate; it was a net-positive investment. At the same time, its politically motivated redesign sacrificed roughly one-third to one-half of its potential gains. Political priorities thus measurably redirected economic activity away from more productive locations.

Our study speaks to several literatures. Our primary contribution is to apply the market access approach from spatial economics (e.g., Redding, Sturm and Wolf, 2011; Ahlfeldt et al., 2015; Donaldson and Hornbeck, 2016; Allen and Arkolakis, 2023) to a common political economy phenomenon. Politics-induced infrastructure is widespread across countries and eras, from colonial railroads built for military control (Jedwab and Moradi, 2016) to roads that reward the president's own ethnic group (Burgess et al., 2015), yet their aggregate costs remain far less quantified than

[2]These estimates remain similar when we exclude all grid cells that ever contained a national capital, indicating that the effects operate through transportation networks induced by capital relocation rather than through the capitals themselves.

their local benefits. In doing so, we join a broader literature on how political institutions shape economic development, such as local state capacity in Vietnam (Dell, Lane and Querubin, 2018), and colonial institutions in Java (Dell and Olken, 2020).

A related literature studies the political and economic consequences of capital cities: dictatorial and closed regimes have abnormally large capital cities (Ades and Glaeser, 1995), isolated capitals are associated with worse governance (Campante and Do, 2014; Campante, Do and Guimaraes, 2019), and economic advantages of capital cities did not necessarily persist in China (Bai and Jia, 2023). Using a spatial framework, Morten and Oliveira (2024) show that roads connecting a newly built capital can generate large welfare gains. Our study highlights a tradeoff that has been less studied: the same politically motivated infrastructure that raises aggregate economic activity can simultaneously misallocate it.

A complementary literature studies the reverse relationship: geography shaping political institutions, from river shifts that gave rise to early governments (Allen, Bertazzini and Heldring, 2023) to the geography separating modern national borders (Allen, 2023). Our findings suggest that there could be a mutual relationship between politics and geography.

Finally, the Grand Canal may be the most important state infrastructure in Chinese history and has been studied by an interdisciplinary literature (e.g., Huang, 1918; Elvin, 1973; Fu, 1985; Yao, 1998; Zhang and Lenzer, 2020; Huang et al., 2021; Cao and Chen, 2022). We draw on them when discussing the background in Section 2.

2 Historical Background and Data

2.1 Historical Background

Since antiquity, China has relied on an extensive network of roads, natural rivers, and canals to connect its territory to its political center. As early as the Qin dynasty (221-206 BC), the first "national roads" radiated outward from the capital Xianyang, complemented by a system of courier stations that transmitted information and reinforced central control (Chen and Li, 2023).

National capital relocation Each dynasty in our sample had a capital of its own, often reflecting the ruling house's own power base. The Tang (618–907) ruled from Chang'an (modern Xi'an), home to the aristocratic clans from which its founders emerged, with Luoyang periodically serving

as a secondary capital. The Song (960–1279) chose Kaifeng as its capital: Zhao Kuangyin, the founding emperor of Song, was stationed there. Chang'an, Luoyang, and Kaifeng all sat in or near the central plain. The Mongol-founded Yuan (1271–1368) broke this pattern, moving the capital far to the north, to Beijing, close to the Mongols' own steppe power base. The Ming (1368–1644) began at Nanjing, in the Yangtze delta's economic heartland, but the Yongle Emperor, who had ruled the north before seizing the throne, relocated the capital to his own power base in Beijing in the 1420s. The Manchu-founded Qing (1644–1912), whose homeland lay in the northeast, kept the capital there.

The Grand Canal Small, local canals were progressively connected and expanded into a national waterway network, a process largely completed by the Sui Dynasty (581-618 CE), first for military transport and, increasingly, for moving tribute grain that helped sustain political centralization and unity in imperial China (Zhang and Lenzer, 2020). As long as the capital remained in or near the central plain, this network needed only incremental adjustment: Emperor Yang of Sui, for instance, excavated the Guangji Canal so that the network would run through his new capital at Luoyang, and the same basic route, connecting north, center, and south, continued to serve Chang'an under the Tang and Kaifeng under the Song. What began as a military project became, after the mid-Tang, the fiscal lifeline of the regime as it grew more dependent on the Yangtze-Huai river basin in the south (Huang et al., 2021).

When the newly founded Yuan dynasty reunified China in 1271, it chose Beijing, close to the Mongols' own steppe power base, as its capital. To connect this capital to the Yangtze Delta, by then the country's economic center, the Yuan rebuilt the canal between 1283 and 1293, digging the Jizhou and Huitong Canals to create a direct Beijing-Hangzhou route through Shandong that bypassed the central plain entirely (Yao, 1998). During this redesign, the new route was just over 1,700 kilometers, roughly 900 kilometers shorter than its Sui-Tang predecessor. Kaifeng lost its role as a transportation hub and receded into an ordinary provincial town. The Ming and Qing dynasties, whose capitals also sat at or near Beijing, maintained this route, moving some 3.5 million quintals of rice a year in the early 19th century, an unprecedented scale for the time (Huang, 1918; Elvin, 1973). The Grand Canal started declining with the rise of sea shipping and was gradually abandoned by the mid-19th century (Cao and Chen, 2022).

In sum, the canal's route was drastically redrawn once over our sample period, exactly when the capital relocated from the central plain to Beijing under the Yuan. This gives us sharp, quasi-experimental variation: the same underlying geography supported two starkly different canal routes,

one connecting north, center, and south before 1271, and one connecting only north and south, bypassing the center, afterward.

2.2 Data

Scope of space and time The spatial scope of this article is equivalent to "China proper", that is, the regions south of the Great Wall, accounting for approximately 90% of the country's population in the late Qing Dynasty (Ge, 2000). We divide the area into 361 grids with a grid size of 1 degree × 1 degree. Our census data spans five dynasties (Tang, Song, Yuan, Ming, Qing) ranging from 741 to 1820. The shock we study is the Yuan dynasty's relocation of the capital from central China to Beijing in the north in 1271. The long panel allows us to trace the changes before and after the relocation shock.

Appendix Table A.1 lists the summary statistics and sources of the variables. Below, we summarize the key data.

Population Our main measure of economic development is population density during 741-1820 CE, which can be obtained based on information on population size and geographical area in each grid. We collected population information from Ge (2000) and Liang (2008) and converted it into a grid population based on the overlap area between the grid and different regions for each sample period (see details in Appendix A.1). The census data is available for nine periods: 741, 980, 1080, 1102, 1290, 1393, 1580, 1776, and 1820. We finally have a nine-period balanced panel for population across 361 grids.

Market access We digitize the waterway and land-route networks of the five dynasties from the *Historical Maps of China* (Cheng and Xu 1980). Figure 2 maps all five networks, highlighting the Song and Ming in particular since they bracket the Grand Canal's rerouting. Following Donaldson and Hornbeck (2016), we first approximate a grid's market access and then use a spatial framework to derive a model-based measure. Grid o's market access is defined as the population of every other grid d, discounted by the cost of reaching it:

$$MA_o = \sum_{d \neq o} \tau_{od}^{-\theta} L_d \tag{1}$$

where population (L_o) is excluded from the summation because it is itself co-determined by market

access; we also show robustness to proxying L_d with the Caloric Suitability Index (CSI), a measure of potential crop yield unaffected by this concern. Section 4.2 derives this expression from a general equilibrium trade model.

Two inputs remain: the trade cost matrix τ_{od} and the trade elasticity θ. We construct τ_{od} as the minimum-cost route between every pair of grids in each sample year, using cost rates calibrated separately for the Grand Canal, natural waterways, land routes, and trails from historical transport records (Appendix A.2 details the network construction and cost calibration). The calibrated rates are 0.157 tons of grain consumed per ton shipped 1,000 km for natural waterways, 0.249 for the Grand Canal, 0.965 for land roads, and 6.087 for trails: natural waterways are cheapest because they draw on tides and wind, the Grand Canal costs more because it relies on human towing power, and land transport is costlier still, with trails, reliant on pack animals rather than carriages, the most expensive mode of all.

θ governs how sharply market access declines with distance: a lower θ implies more dispersed productivity and stronger trade motives across grids. Existing estimates range from 3.60 to 12.86, with Eaton and Kortum (2002) preferring 8.28 and Donaldson and Hornbeck (2016) estimating 8.22 for the 19th-century United States. We instead estimate $\theta = 8.62$ directly from our data via Nonlinear Least Squares (Section D.2), with a bootstrapped 95% confidence interval of [8.08, 9.04], and show our results are robust to alternative values.

We compute market access for each grid in each of our nine sample periods. These period-to-period changes are substantial and reflect two forces: population growth and network change. Holding population fixed at its pre-1500 CSI-based level isolates the network-driven component; by far the largest such change occurs between 1102 and 1290, exactly the Song-Yuan window in which the canal was rerouted (Appendix Figure A.2.b).

Other grid-level characteristics The development of historical regional economies largely depends on the local geographical environment and the suitability of major crops. Therefore, we control for a rich set of geographical conditions and agricultural suitability variables in our estimates. Geographic variables include whether the grid has plains, major rivers, whether it is located on the coast, the macro-region it belongs to, the grid's average slope, elevation, grid area, and centroid longitude and latitude. Agricultural variables include suitability of wheat, rice, fox millet, maize and sweet potato.

3 The Canal Follows the Capital: Identification and Evidence

The Grand Canal's stated purpose was to move troops, tribute grain, and officials between the capital and the country's military frontier in the north and economic core in the south, not to minimize the cost of trade. When the capital relocated, the route that best served this political purpose changed accordingly. We test whether this optimal route to reach the capital predicts where the canal was actually built.

Relevance of the optimal route To construct the optimal route to the capital, we use a Digital Elevation Model (DEM) to identify terrain too mountainous for canal excavation, defined as terrain above the highest elevation the historical canal actually reached. We then draw the shortest path avoiding this terrain through a fixed set of waypoints: a northern terminus, a turning point in the central plain (relevant only before the Yuan relocation), and southern termini at Yangzhou and Hangzhou (Appendix B.1).

Appendix Figure B.1 plots this optimal route against the actual canal (Song and Ming shown as examples): the two line up closely, suggesting the actual Grand Canal can be read as the least-cost route connecting the north, the south, and wherever the capital happened to be.

We confirm this formally by estimating

$$Waterway_{it} = \alpha_0 OptimalRoute_{it} + \sum_{t=1}^{t=9} (Z_i \times I_{\rho=t})\gamma^{\rho} + \lambda_i + \eta_t + \epsilon_{it} \tag{2}$$

where $Waterway_{it}$ is the length of the actual waterway in grid i in year t, or an indicator for whether one passes through it, and $OptimalRoute_{it}$ is the corresponding length or presence of the optimal route.

The specification includes grid and year fixed effects. Z_i is a set of control variables on grid's time-invariant geographical conditions and agricultural suitability as described in Section 2.2, and we allow their influence to vary over time by interacting with year fixed effects. The standard errors are clustered at the grid level. These controls and clustering are used consistently in the following specifications as well.

As shown in Table 1 (Panel A), a 1-kilometer increase in the optimal route raises the actual waterway by about 0.87 kilometers, and grids on the optimal route are correspondingly more likely to contain an actual waterway. Both results are stable whether or not we include the full set of

geographic and agricultural controls.

We also use this optimal network to construct two market access measures that are plausibly exogenous to both route selection and population growth: one weights the optimal network's trade costs by each grid's Tang-dynasty population, $MA_{it}^{opt,TangPopu}$, and the other by its Caloric Suitability Index measured before 1500 (i.e., before Columbian Exchange), $MA_{it}^{opt,csi}$, a proxy for the population the grid could support, fixed well before the outcomes we study. We then regress actual, population-weighted market access on these two measures indicated by MA_{it}^{opt,pop_0} below:

$$\ln MA_{it} = \alpha \ln MA_{it}^{opt,pop_0} + \sum_{t=1}^{t=9} (Z_i \times I_{\rho=t})\gamma^{\rho} + \lambda_i + \eta_t + \epsilon_{it}. \tag{3}$$

As reported in Table 1 (Panel B), we find a strong, significant relationship: a 1% increase in either instrument raises actual market access by about 0.53%, consistent with the optimal network capturing a real, quantitatively important share of the variation in realized market access. For robustness, we consider alternative values of θ (Table B.2.a) and alternative cost parameters (Table B.2.b) when constructing market access. Overall, these results show that the canal follows the capital, and so does the market access it generates.

Placebo tests A natural concern with the result above is that the optimal route may simply trace terrain that is cheap to build on for any purpose, coincidentally correlated with the capital's location, rather than capturing the specific political objective of connecting to whichever city was capital. Because our panel spans the 1271 relocation, we can address this concern directly: if the optimal route were merely picking up generically favorable geography, its predictive power should be stable across dynasties; if it instead captures the political motive, its predictive power should track the capital itself and switch exactly when the capital does. We separately compute each grid's optimal route *to the Song capital* and *to the Yuan capital*, interact both with a full set of dynasty dummies, and trace out their predictive power on the actual waterway dynasty by dynasty. As reported in Appendix B.3, the route to the Song capital predicts the waterway well through the Tang and Song, reflecting the fact that the capitals, despite relocation were located in the central plain. This optimal route loses its power exactly when the capital moves to Beijing. Similarly, the route to the Yuan capital shows the mirror-image pattern, gaining predictive power only from the Yuan onward.

4 Benefits and Costs of Politics-Driven Market Access

We now turn to the economic consequences of the canal's politically motivated design. We proceed in two steps. We first show, in reduced form, that market access raises population density, establishing the channel through which the canal's route shapes economic geography. We then embed this relationship in a structural spatial equilibrium model to ask two counterfactual questions: how much did the Grand Canal contribute to aggregate welfare, and how much welfare was lost because its route was redrawn around political priorities rather than economic ones.

4.1 Reduced-Form Evidence: Market Access and Population Density

Main results We begin with an OLS specification that regresses log population density in grid i and year t on log market access:

$$\ln PopDensity_{it} = \beta \ln MA_{it} + \sum_{t=1}^{t=9} (Z_i \times I_{\rho=t})\gamma^{\rho} + \lambda_i + \eta_t + \epsilon_{it}. \tag{4}$$

The specification includes grid and year fixed effects, so β is identified off within-grid changes in market access over time, net of any time-varying return to a grid's geographic and agricultural endowments.

Population and canal placement may nonetheless be jointly determined: already-prosperous grids could attract routes, or unobserved local shocks could drive both variables together, biasing the OLS estimate in either direction. To address this, we instrument $\ln MA_{it}$ with $\ln MA_{it}^{opt,pop_0}$, the market access implied by the optimal route to the capital from Section 3, weighted by a measure of each grid's population capacity fixed well before the outcomes we study, pop_0: either its Tang-dynasty population or its pre-1500 Caloric Suitability Index. Because this instrument is built from a route chosen to serve the capital rather than to minimize trade costs, and is weighted by a pre-determined population measure, it is plausibly uncorrelated with the contemporaneous shocks that would bias the OLS estimate.

Table 2 reports the results. The OLS estimate in column (1), with only grid and year fixed effects, implies that a 1% increase in market access raises population density by approximately 0.18%. Adding the full set of geographic and agricultural controls in column (2) lowers this only modestly, to 0.14%, indicating the relationship is not simply an artifact of omitted, time-varying geographic advantage. The IV estimates in columns (3)-(6) are, comparable to the OLS

estimate: 0.16% using the CSI-weighted instrument and 0.24% using the Tang-population-weighted instrument. The first stage is strong in both IV specifications, with F-statistics well above 100 in every column.

A threat to our IV strategy is that the optimal route to the capital could predict direct, place-based state investment, such as garrisons, courier and postal relay stations, grain-transfer warehouses, rather than working solely through market access. Because such investment should raise population locally, in grids on or beside the route, rather than through a grid's broader access to distant markets, we address this concern by progressively excluding first-order neighboring grids (within approximately 100 km) and second-order neighboring grids (within approximately 200 km) from the market access calculation, reconstructing both the actual market access regressor and the optimal-route-based instrument this way. The results show that market access to more distant regions still significantly contributes to local population growth, for both the OLS and IV specifications (Appendix C.1).

Event study: The Song-Yuan Canal redesign We further examine how the population density is affected by the sudden change in market access caused by the shortening of the Grand Canal after the Song Dynasty. We define a "market access shock" as the actual market access in 1102 minus that in 1290, and estimate its annual impact on population density by interacting this shock with a full set of period dummies.

Grids where the rerouting caused a larger loss of market access should, given the positive elasticity documented above, experience a corresponding decline in population density, and this is exactly what we find: the interaction coefficient shows no differential pre-trend before 1102, then turns negative and significant precisely in 1290, the period the rerouted canal came into use, with a magnitude of -0.176. The effect does not fade with time: it remains negative and of similar magnitude (between -0.2 and -0.1) through 1393 and every subsequent sample year, indicating that the shock's impact on population density is permanent rather than transitory. This pattern, in which the effect emerges exactly when the canal was rerouted, carries the sign implied by the positive market-access elasticity, and never reverts, is consistent with the redesign having durably relocated economic activity away from the grids it stopped serving, rather than merely causing a temporary disruption that later recovered. Appendix C.2 presents the full results of this event study, including a robustness check that isolates the canal-driven component of the shock using pre-1500 CSI in place of population.

Robustness checks We probe the robustness of this result along three dimensions. The detailed discussions on these additional checks are shown in Appendix C.3.

First, the result is robust to alternative measurement choices: a set of values of θ (the trade elasticity) and alternative transportation cost settings (Table C.3.a); market access based on the Caloric Suitability Index (CSI), a relatively exogenous indicator of grid population (Table C.3.b); and alternative instrumental variables built from different definitions of the optimal route to the national capital: one minimizing travel time using the Human Mobility Index (Özak, 2018), and one taking the shortest straight-line path between major locations, in place of the DEM-based least-cost route used in the baseline (Table C.3.c).

Second, we account for confounding shocks that could independently drive population density over this period, unrelated to market access: Sino-nomadic warfare, which caused a sharp decline in the population of the Central Plains (Table C.3.d); and the political status of the provincial capital, which could raise local population density by improving the local transportation network rather than through the canal itself (Table C.3.e).

Third, we address endogeneity concerns in the market access measure itself: the possibility that land routes are endogenously drawn toward already-prosperous grids, which we address by controlling for the length of land routes in and around each grid (Table C.3.f).

4.2 Counterfactual Analysis Based on a Spatial Framework

The reduced-form estimates above show that market access matters for population density, but they cannot tell us how much the canal itself, or its politically motivated redesign, was worth in the aggregate. To answer these questions, we embed market access in a general equilibrium trade model following Eaton and Kortum (2002) and Donaldson and Hornbeck (2016). Building this model is not our main contribution, so we discuss the key idea here and relegate the full derivation to Appendix D.1.

The setup is simple: land is immobile, labor and capital are mobile across grids, production is Cobb-Douglas, and productivity is Fréchet-distributed with dispersion parameter θ, the same trade elasticity that enters our market access measure. Of course, labor was unlikely to be perfectly mobile in imperial China. This is less of a concern for our purposes for two reasons: our sample periods span entire dynasties, long enough for population to adjust across generations even if migration was still imperfectly mobile; and our counterfactuals below always compare outcomes computed under this same mobility assumption, so what matters is the relative difference between

scenarios rather than the absolute level implied by any one of them.

Under CES preferences and iceberg trade costs τ_{od}, Eaton and Kortum (2002) show that the resulting price index in grid d and the value of trade flows from grid o to grid d both take closed forms in $(A_o, \tau_{od}, q_o, w_o)$. Aggregating trade flows across destinations, imposing goods-market clearing, and assuming symmetric trade costs, following Donaldson and Hornbeck (2016), collapses these expressions into a single market-access recursion,

$$MA_o = \rho \sum_d \tau_{od}^{-\theta} MA_d^{-(1+\theta)/\theta} L_d, \tag{5}$$

for a proportionality constant $\rho > 0$. Equation (5) is the model-consistent counterpart of the approximation in equation (1) (Section 2.2): both discount each destination by trade cost raised to the power $-\theta$, but here a destination's pull is summarized by its own equilibrium market access MA_d rather than by its raw population, with the exponent on L_d pinned down by the model rather than assumed. Appendix D.1 spells out every intervening step, including the price index and gravity equation this recursion is built from.

The key insight is that solving this model for the labor-mobile equilibrium delivers the same log-linear relationship between population and market access that we estimated in reduced form,

$$\ln L_o = \text{const} + \frac{1 + \theta(1 + \alpha + \gamma)}{\theta(1 + \theta\alpha)} \ln MA_o, \tag{6}$$

except that here the elasticity is not a free parameter: it is a known function of three structural parameters, where α and γ denote land's and labor's income shares in production. This structural elasticity is pinned down by calibrated parameters and is what we use to solve the counterfactuals below.

Following the literature, we separately verify that reduced-form estimates constructed from the model-consistent market access track those from the simple approximation. As shown in Appendix Table D.3, when we instrument for market access and used standardize the two sets of market access measures, we obtain similar elasticities.

Based on research on historical China (Brandt, 1989; Perkins, 2017), we set $\alpha = 0.4$ and $\gamma = 0.55$. The land share estimated for historical China exceeds the corresponding estimate of 0.19 from modern cross-country data in Caselli and Coleman (2001), consistent with the greater importance of land in our agricultural setting.[3] The labor share is comparable to the estimate in

[3] If we use 0.19 as the estimate, the Grand Canal would raise aggregate population by 4-10%, higher than our current

Donaldson and Hornbeck (2016). We estimate $\theta = 8.62$ by fitting this equation to our data via nonlinear least squares (Appendix D.2).[4]

Counterfactual without the Canal: the Grand Canal raised aggregate population Computing a counterfactual then takes two further steps, which we summarize here and derive fully in Appendix D.4. First, we do not observe each grid's underlying productivity or land quality directly, so we back them out from the data: given the actual transportation network and actual population in each sample year, the model's equilibrium conditions imply a unique combination of productivity and land endowment for every grid that is consistent with what we observe. Second, because these grid-level fundamentals reflect geography and technology rather than the transportation network, we hold them fixed and replace the actual network with a counterfactual one (removing the canal, say, or swapping in another dynasty's route) and re-solve the same equilibrium conditions for the population distribution this counterfactual network implies. The difference between this counterfactual population and the actual population is our estimate of the effect in question.

We first drop the Grand Canal from the transportation network entirely and re-solve the model for the counterfactual population this implies (Table 3, Panel A). The loss is sizable from the Tang through the Ming: aggregate population would have been 5.47% lower in 741 (Tang), 4.95–5.10% lower across 980–1102 (Song), 5.56% lower in 1290 (Yuan), and 5.98–6.12% lower in 1393–1580 (Ming) had the canal never existed. This loss then falls by more than half in the Qing, to 2.51% in 1776 and 2.50% in 1820. This break around the 18th century lines up with the canal's historical decline as sea shipping rose and progressively took over the tribute-grain trade the canal once carried (Section 2).

To make sure that the counterfactual results are driven by the transportation networks rather than the changes in the productivity or attractiveness of capital locations, we repeat the counterfactual analysis after dropping the ever-capital grids in Appendix D.5 and find similar estimates.

As a benchmark, we also project these counterfactual impacts directly using our baseline reduced-form elasticity (Table 2, Column 2) as a partial-equilibrium reference. As reported in Panel A of Table D.6.a, the reduced-form projections yield larger aggregate losses: 9.26% in 741 (Tang), 6.23–6.42% across 980–1102 (Song), 7.74% in 1290 (Yuan), 8.47–8.54% across 1393–1580 (Ming), and 3.38–3.40% in 1776–1820 (Qing). These results indicate that the reduced-form

estimates.

[4]The structural elasticity is 0.46, higher than our reduced-form estimates (0.14-0.24), reflecting population is not perfectly mobile. The difference is already noted in Donaldson and Hornbeck (2016).

projections omit network-wide reallocation through the market-access recursion (Equation (5)).

We next ask how much cheaper land transport would have needed to become (say, because the empire redirected the resources spent building and maintaining the canal toward roads instead) to fully offset the loss from dropping the canal, and we find that the answer tracks the same before/after-18th-century divide documented above (Table 3, Panel A). For the Qing, whose reliance on the canal was already modest, a 20% reduction in land transport costs is more than enough: aggregate population would in fact be slightly higher than under the actual network. For the Tang through the Ming, when the canal carried most interior trade, offsetting the loss requires a much larger, 40% reduction in land transport costs. The reduced-form projections exhibit the a similar historical divide in offsetting these losses through cheaper land transport (Table D.6.a, Panel A).

Counterfactual of Canal location: political redesign caused misallocation Having shown the canal itself was valuable, we next ask whether its specific route, redrawn around political priorities when the Yuan relocated the capital to Beijing, was also the economically best one. We swap each dynasty's actual canal for another dynasty's route, holding the rest of that dynasty's network fixed, and re-solve for the counterfactual population (Table 3, Panel B).

The results split cleanly around the 1271 relocation, the same divide documented in the first counterfactual. Before 1271, substituting in either of the two routes built after the relocation (the Yuan's own, or the Ming/Qing route it evolved into), both of which bypassed the central plain, always lowers population: doing so costs 1.17–3.28% in 741 (Tang) and 1.57–4.17% in 980–1102 (Song), with the loss more than doubling once the canal is restricted to the direct Beijing-Hangzhou alignment. After 1271, the opposite holds: substituting in either pre-relocation route (the Tang's or the Song's), both of which ran through the central plain, always raises population, by 1.07–1.37% in 1393–1580 (Ming) and by 1.39–2.17% in 1776–1820 (Qing).[5] One further pattern confirms this reading: substituting the Yuan's own route into the Ming or Qing network barely moves population, by only 0.06%–0.23%, because the Ming and Qing, as discussed in Section 2, essentially kept the Yuan's direct Beijing-Hangzhou alignment in place.

This qualitative pattern is echoed by our reduced-form counterfactual projections (Table D.6.a,

[5]In addition, if the Song dynasty adopted the Tang dynasty's canal, its population would decrease. This is because, although the Tang canal route is roughly similar to that of the Song, it is simpler and less developed. Furthermore, the Yuan dynasty's population would decline if it adopted the Tang or Song Grand Canal. This is plausibly because our procedure backs out each grid's productivity from that period's *actual* population: the Sino-nomadic wars of 1211–1279 (Appendix C.3) had temporarily depressed population in the Central Plains by 1290. Routing the canal back through the Central Plains would thus connect low-productivity regions.

Panel B). Once again, relying on reduced-form alone, route swaps across dynasties yield similar directional shifts but larger magnitudes. For instance, substituting post-1271 routes into pre-1271 dynasties persistently reduces aggregate population—by 1.48–5.36% in 741 (Tang) and 1.99–5.11% in 980–1102 (Song). We report additional counterfactuals under alternative transport cost assumptions in Tables D.6.b and D.6.c for the general equilibrium model and the reduced-form projections, respectively.

In sum, the Yuan relocation measurably reallocated economic activity away from where it would otherwise have been, and that misallocation persisted for as long as later dynasties kept the Yuan's route.

5 Conclusion

Politically motivated infrastructure, such as capitals anchoring rail and road networks, colonial railroads built for military control, roads that favor a leader's home region, is common across countries and eras, yet its aggregate costs have rarely been separated from its local benefits. Understanding both aspects in the same framework is our main motivation.

In this paper, we use China's Grand Canal to study this tradeoff. The canal's route was redrawn dramatically exactly when the Yuan dynasty relocated the capital from the central plain to Beijing, giving us sharp variation in the canal's route that is plausibly exogenous to the underlying geography and population of the regions it served. We show that this politically motivated redesign had important consequences for economic geography: the canal's route shaped market access, which in turn shaped population distribution. Embedding these estimates in a spatial framework, we show that the canal created real economic value in the aggregate, but its politically motivated route also led to sizable misallocation.

These findings illustrate a general point: politically motivated infrastructure can be genuinely valuable in the aggregate and still misallocate resources within that aggregate, because the same political motive that gets it built also shapes where, specifically, it goes. This tradeoff is not visible from local benefits alone, and it is likely to recur wherever transportation networks are anchored to political rather than economic centers, in China's past or elsewhere today.

References

Ades, Alberto F, and Edward L Glaeser. 1995. "Trade and Circuses: Explaining Urban Giants." *The Quarterly Journal of Economics*, 110(1): 195–227.

Ahlfeldt, Gabriel M., Stephen J. Redding, Daniel M. Sturm, and Nikolaus Wolf. 2015. "The Economics of Density: Evidence from the Berlin Wall." *Econometrica*, 83(6): 2127–2189.

Alder, Simon. 2025. "Chinese Roads in India: The Effect of Transport Infrastructure on Economic Development." *Journal of International Economics*, 157: 104140.

Allen, Robert C., Mattia C. Bertazzini, and Leander Heldring. 2023. "The Economic Origins of Government." *American Economic Review*, 113(10): 2507–2545.

Allen, Treb. 2023. "The Topography of Nations." NBER Working Paper 31795, Cambridge, MA.

Allen, Treb, and Costas Arkolakis. 2023. "Economic Activity Across Space: A Supply and Demand Approach." *Journal of Economic Perspectives*, 37(2): 3–28.

Bai, Ying, and Ruixue Jia. 2023. "The Economic Consequences of Political Hierarchy: Evidence from Regime Changes in China, 1000–2000 CE." *Review of Economics and Statistics*, 105(3): 626–645.

Balboni, Clare. 2025. "In Harm's Way? Infrastructure Investments and the Persistence of Coastal Cities." *American Economic Review*, 115(1): 77–116.

Brandt, Loren. 1989. *Commercialization and Agricultural Development: Central and Eastern China, 1870–1937.* Cambridge University Press.

Burgess, Robin, Remi Jedwab, Edward Miguel, Ameet Morjaria, and Gerard Padró i Miquel. 2015. "The Value of Democracy: Evidence from Road Building in Kenya." *American Economic Review*, 105(6): 1817–1851.

Campante, Filipe R, and Quoc-Anh Do. 2014. "Isolated Capital Cities, Acountability, and Corruption: Evidence from US States." *American Economic Review*, 104(8): 2456–2481.

Campante, Filipe R., Quoc-Anh Do, and Bernardo Guimaraes. 2019. "Capital Cities, Conflict, and Misgovernance." *American Economic Journal: Applied Economics*, 11(3): 298–337.

Cao, Yiming, and Shuo Chen. 2022. "Rebel on the Canal: Disrupted Trade Access and Social Conflict in China, 1650–1911." *American Economic Review*, 112(5): 1555–1590.

Caselli, Francesco, and Wilbur John Coleman. 2001. "Cross-Country Technology Diffusion: The Case of Computers." *American Economic Review*, 91(2): 328–335.

Cheng, Guangyu, and Shengmo Xu. 1980. *Zhongguo Lishi Ditu [Historical Maps of China].* Taipei: Chinese Culture University Press.

Chen, Xiangming, and Ziming Li. 2023. "Xi'an: From an Ancient World City to a 21st-Century Global Logistics Centre." In *Routledge Handbook of Asian Cities*. 172–186. London: Routledge.

China's Military History Editorial Committee. 2003. *Zhongguo Lidai Zhanzheng Nianbiao [Chronology of Wars in China].* . 2nd ed., Beijing: PLA Press.

Dell, Melissa, and Benjamin A. Olken. 2020. "The Development Effects of the Extractive Colonial Economy: The Dutch Cultivation System in Java." *Review of Economic Studies*, 87(1): 164–203.

Dell, Melissa, Nathan Lane, and Pablo Querubin. 2018. "The Historical State, Local Collective Action, and Economic Development in Vietnam." *Econometrica*, 86(6): 2083–2121.

De Long, J Bradford, and Andrei Shleifer. 1993. "Princes and Merchants: European City Growth before the Industrial Revolution." *The Journal of Law and Economics*, 36(2): 671–702.

Donaldson, Dave, and Richard Hornbeck. 2016. "Railroads and American Economic Growth: A "Market Access" Approach." *Quarterly Journal of Economics*, 131(2): 799–858.

Duranton, Gilles, Peter M. Morrow, and Matthew A. Turner. 2014. "Roads and Trade: Evidence from the US." *Review of Economic Studies*, 81(2): 681–724.

Eaton, Jonathan, and Samuel Kortum. 2002. "Technology, Geography, and Trade." *Econometrica*, 70(5): 1741–1779.

Elvin, Mark. 1973. *The Pattern of the Chinese Past: A Social and Economic Interpretation.* Stanford, CA: Stanford University Press.

Evans, Laurence. 1984. "Junks, Rice, and Empire: Civil Logistics and the Mandate of Heaven." *Historical Reflections/Réflexions Historiques*, 11(3): 271–313.

Faber, Benjamin. 2014. "Trade Integration, Market Size, and Industrialization: Evidence from China's National Trunk Highway System." *Review of Economic Studies*, 81(3): 1046–1070.

FAO and IIASA. 2012. "Global Agro-Ecological Zones (GAEZ v3.0)." https://iiasa.ac.at/models-tools-data/gaez, Food and Agriculture Organization and International Institute for Applied Systems Analysis.

Fogel, Robert William. 1964. *Railroads and American Economic Growth: Essays in Econometric History.* Baltimore, MD: Johns Hopkins Press.

Fu, Huilan. 1985. *Zhongguo Yunhe Chengshi Fazhan Shi [History of the Development of Canal Cities in China].* Chengdu: Sichuan People's Publishing House.

Galor, Oded, and Ömer Özak. 2016. "The Agricultural Origins of Time Preference." *American Economic Review*, 106(10): 3064–3103.

Ge, Jianxiong. 2000. *Zhongguo Renkou Shi [China Population History].* Shanghai: Fudan University Press.

Harvard-Yenching Institute and Fudan University Center for Historical Geography. 2007. "CHGIS, Version 4." *Database*.

Heblich, Stephan, Stephen J. Redding, and Daniel M. Sturm. 2020. "The Making of the Modern Metropolis: Evidence from London." *Quarterly Journal of Economics*, 135(4): 2059–2133.

Hornbeck, Richard, and Martin Rotemberg. 2024. "Growth Off the Rails: Aggregate Productivity Growth in Distorted Economies." *Journal of Political Economy*, 132(11): 3547–3602.

Huang, Han-Liang. 1918. *The Land Tax in China.* New York, NY: Columbia University Press.

Huang, Wenji, Mingwang Xi, Shibao Lu, and Farhad Taghizadeh-Hesary. 2021. "Rise and Fall of the Grand Canal in the Ancient Kaifeng City of China: Role of the Grand Canal and Water Supply in Urban and Regional Development." *Water*, 13(14): 1932.

Jaworski, Taylor, and Carl T. Kitchens. 2019. "National Policy for Regional Development: Historical Evidence from

Appalachian Highways." *Review of Economics and Statistics*, 101(5): 777–790.

Jedwab, Remi, and Alexander Moradi. 2016. "The Permanent Effects of Transportation Revolutions in Poor Countries: Evidence from Africa." *Review of Economics and Statistics*, 98(2): 268–284.

Liang, Fangzhong. 2008. *Lidai Hukou, Tudi, Tianfu Tongji [Historical Statistics on Hukou, Land and Land Tax of China].* Beijing: Zhonghua Book Company.

Li, Wenzhi, and Taixin Jiang. 1995. *Qingdai Caoyun [Canal Transport in the Qing Dynasty].* Beijing: Zhonghua Book Company.

Morten, Melanie, and Jaqueline Oliveira. 2024. "The Effects of Roads on Trade and Migration: Evidence from a Planned Capital City." *American Economic Journal: Applied Economics*, 16(2): 389–421.

Özak, Ömer. 2018. "Distance to the Pre-industrial Technological Frontier and Economic Development." *Journal of Economic Growth*, 23(2): 175–221.

Perkins, Dwight H. 2017. *Agricultural Development in China, 1368–1968.* Routledge.

Quan, Hansheng, and Richard A. Kraus. 1975. *Mid-Ch'ing Rice Markets and Trade: An Essay in Price History. Harvard East Asian Monographs*, Cambridge, MA: East Asian Research Center, Harvard University.

Redding, Stephen J., Daniel M. Sturm, and Nikolaus Wolf. 2011. "History and Industry Location: Evidence from German Airports." *Review of Economics and Statistics*, 93(3): 814–831.

Yang, Yang. 2018. "Transport Infrastructure, City Productivity Growth and Sectoral Reallocation: Evidence from China." International Monetary Fund, Washington, DC.

Yao, Hanyuan. 1998. *Jing Hang Yunhe Shi [History of the Grand Canal].* Beijing: China Water Resources and Hydropower Press.

Yili Animal Husbandry and Veterinary School of Xinjiang Uygur Autonomous Region. 1979. *Yang Ma Xue [Horse Breeding].* Beijing: Agricultural Press.

Zhang, Mengke, and James H. Lenzer. 2020. "Mismatched Canal Conservation and the Authorized Heritage Discourse in Urban China: A Case of the Hangzhou Section of the Grand Canal." *International Journal of Heritage Studies*, 26(2): 105–119.

Zheng, Piliu, Zhongge Zhang, Xiaohua Chen, and Youren Tu. 1987. *Zhongguo Ma Lv Pinzhong Zhi [Horse and Ass Breeds in China].* Shanghai: Shanghai Science and Technology Press.

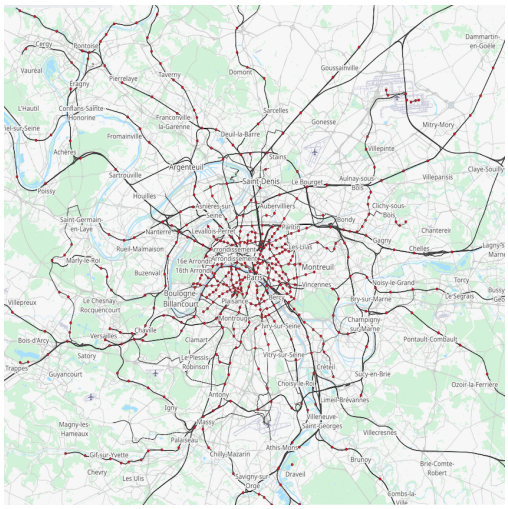
Figure 1: National Capital's Transportation Networks: Examples



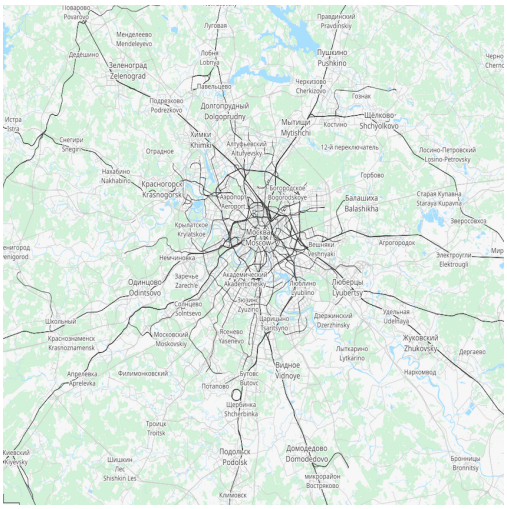
(a) Beijing



(b) New Delhi



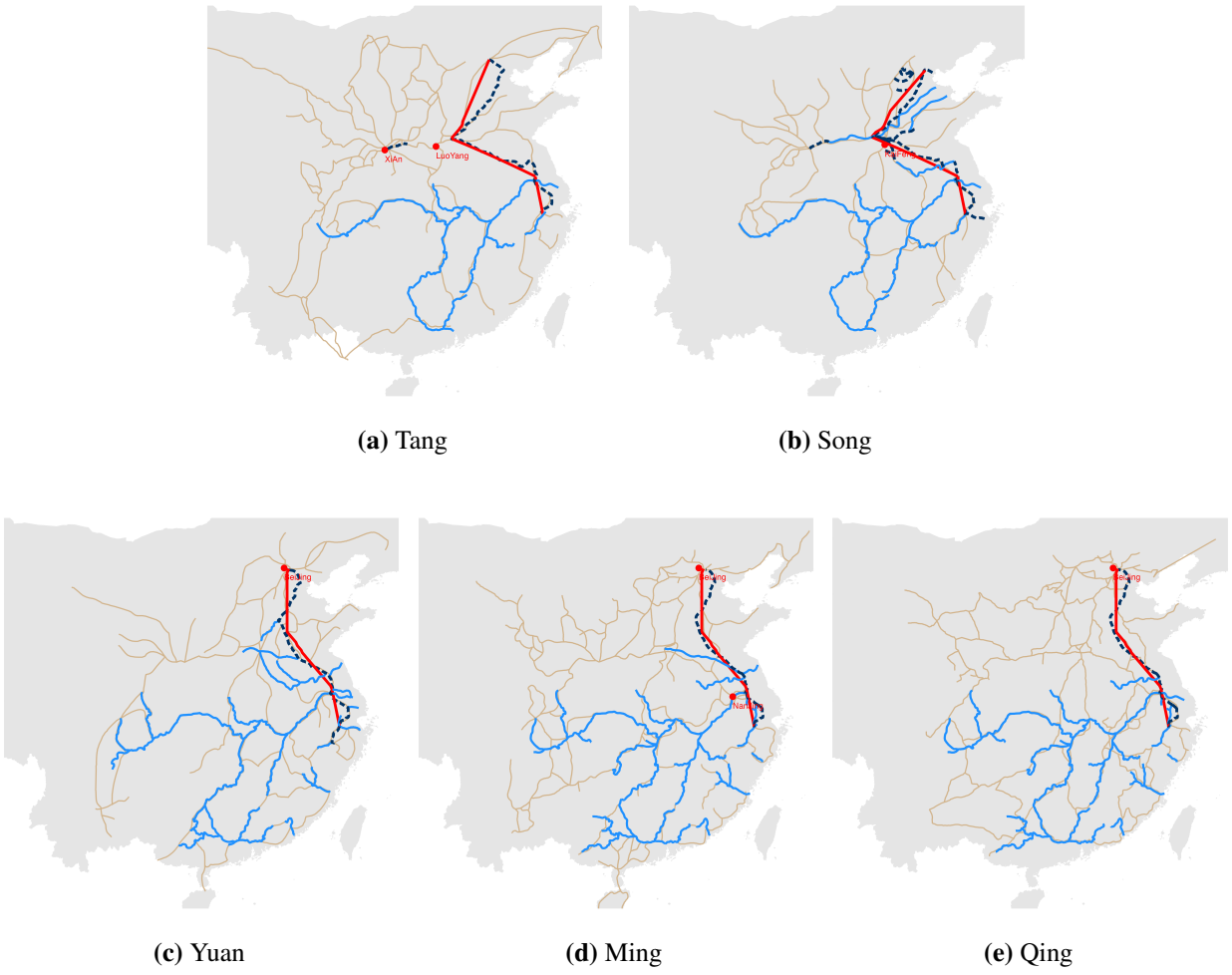
(c) Paris



(d) Moscow

Notes: These maps come from Open Street Map. They illustrate that transportation networks often radiate from the national capital across countries.

Figure 2: National Capital Relocation, Transportation Networks, and Optimal Routes



(a) Tang **(b)** Song

(c) Yuan **(d)** Ming **(e)** Qing

Notes: The brown lines are land routes, the blue lines are waterways, the dashed lines are the actual Grand Canal, and the solid red lines are the optimal route to the national capital (Appendix B.1). The red points are national capitals in each dynasty.

Table 1: Relevance of the Optimal Route

A: Optimal Route Predicts the Actual Waterway				
Dependent variable	Waterway Length		Having Waterway	
	(1)	(2)	(3)	(4)
Optimal Route (DEM)	0.905***	0.868***		
	(0.037)	(0.044)		
Optimal Route (DEM), Indicator			0.846***	0.822***
			(0.038)	(0.041)
Grid FE	Y	Y	Y	Y
Dynasty FE	Y	Y	Y	Y
GeoControl × Dynasty FE		Y		Y
AgriControl × Dynasty FE		Y		Y
R-squared	0.960	0.964	0.947	0.951
Observations	1,805	1,805	1,805	1,805
B: Optimal-Route Market Access Predicts Actual Market Access				
Dependent variable	ln MA			
	(1)	(2)	(3)	(4)
ln MA (optimal, Tang popu.)	0.621***	0.534***		
	(0.037)	(0.041)		
ln MA (optimal, pre-1500 CSI)			0.631***	0.513***
			(0.045)	(0.049)
Grid FE	Y	Y	Y	Y
Year FE	Y	Y	Y	Y
GeoControl × Year FE		Y		Y
AgriControl × Year FE		Y		Y
R-squared	0.873	0.911	0.863	0.906
Observations	3,249	3,249	3,249	3,249

Notes: Panel A regresses the actual waterway on the DEM-based optimal route to the capital (Appendix B.1) in a dynasty-grid panel. Columns (1)-(2) use the length (km) of the actual waterway in the grid as the dependent variable and the length of the optimal route as the regressor; columns (3)-(4) use an indicator for whether the grid contains a waterway. Panel B regresses log actual market access on log market access constructed from the optimal-route network (Equation (3)), weighted by each grid's Tang-dynasty population (columns (1)-(2)) or its pre-1500 Caloric Suitability Index (columns (3)-(4)), in a grid-year panel. Controls include the grid's average slope, elevation, area, and centroid coordinates; whether the grid has plains, major rivers, or coastline and its macro-region; and the suitability of wheat, rice, fox millet, maize, and sweet potato, all interacted with year fixed effects. Standard errors displayed in parentheses are clustered at grid level. *** $p < 0.01$, ** $p < 0.05$, * $p < 0.1$.

Table 2: Market Access and Population Density

Dependent variable	ln Popu. Density					
	(1)	(2)	(3)	(4)	(5)	(6)
	OLS		IV: ln MA (optimal, pre-1500 CSI)		IV: ln MA (optimal, Tang popu.)	
ln MA	0.180***	0.143***	0.124***	0.159***	0.187***	0.239***
	(0.022)	(0.018)	(0.040)	(0.045)	(0.038)	(0.043)
Grid FE	Y	Y	Y	Y	Y	Y
Year FE	Y	Y	Y	Y	Y	Y
GeoControl × Year FE		Y		Y		Y
AgriControl × Year FE		Y		Y		Y
KP F-stat			200.17	110.67	285.91	170.78
R-squared	0.805	0.891	0.062	0.049	0.069	0.028
Observations	3,249	3,249	3,249	3,249	3,249	3,249

Notes: The dependent variable is log population density. Column (1) reports the OLS estimate with grid and year fixed effects only; column (2) adds the full set of geographic and agricultural controls, interacted with year fixed effects, as listed in Table 1. Columns (3)-(4) and (5)-(6) report the corresponding IV estimates, instrumenting for ln MA with market access constructed from the politically optimal route to the capital (Section 3), weighted respectively by each grid's pre-1500 Caloric Suitability Index (columns (3)-(4)) and by its Tang-dynasty population (columns (5)-(6)); see Equation (3). Standard errors displayed in parentheses are clustered at grid level. *** $p < 0.01$, ** $p < 0.05$, * $p < 0.1$.

Table 3: Counterfactual Estimates: Dropping and Relocating the Grand Canal

	Popu. Changes (%)								
Year	741	980	1080	1102	1290	1393	1580	1776	1820
	(1)	(2)	(3)	(4)	(5)	(6)	(7)	(8)	(9)
A. Drop the Grand Canal									
Land Road Cost Unchanged	-5.47	-5.02	-5.10	-4.95	-5.56	-5.98	-6.12	-2.51	-2.50
Land Road Cost Decline 20%	-3.02	-2.94	-3.07	-2.95	-3.27	-3.57	-3.60	0.23	0.22
Land Road Cost Decline 30%	-1.37	-1.60	-1.76	-1.65	-1.77	-2.03	-1.99	2.00	1.97
Land Road Cost Decline 40%	0.71	0.04	-0.16	-0.07	0.05	-0.17	-0.05	4.13	4.09
Land Road Cost Decline 50%	3.35	2.12	1.89	1.95	2.32	2.10	2.33	6.78	6.70
B. Adopt Grand Canal in Other Dynasty									
Adopt Grand Canal in Tang Dynasty		-1.61	-2.03	-1.95	-0.80	1.07	1.37	1.39	1.44
Adopt Grand Canal in Song Dynasty	1.31				-1.70	1.27	1.24	2.17	2.13
Adopt Grand Canal in Yuan Dynasty	-1.17	-1.64	-1.57	-1.60		0.07	0.06	0.20	0.23
Adopt Grand Canal in Ming/Qing Dynasty	-3.28	-4.17	-3.96	-3.86	-1.74				

Notes: This table reports the percentage change in aggregate population, relative to the actual population, implied by counterfactual transportation networks solved from the structural model (Appendix D.1), holding each grid's productivity and land endowment fixed at the levels backed out from the actual network and actual population in that sample year. Each column corresponds to one of the nine census years, with the rest of that year's network held at its actual configuration. Panel A drops the Grand Canal from the network entirely, under alternative assumptions about how much land-route costs would have fallen had the empire redirected investment from the canal to overland routes (0-50% cost declines relative to the baseline rate). Panel B replaces the actual canal in a given year with another dynasty's actual canal route, holding the rest of that year's network fixed; rows indicate the donor dynasty whose canal route is substituted in, and blank cells correspond to years in which the donor dynasty's own route was already in use.

Appendix A Data Construction

Table A.1: Summary Statistics & Data Sources

Variable	Obs.	Mean	S.D.	Sources
1.Economic Outcome				
ln Popu. Density	3249	2.750	1.525	A
2. Market Access				
ln MA	3249	11.589	2.437	A,B
ln MA (optimal, Tang popu.)	3249	9.371	2.605	A,B
ln MA (optimal, pre-1500 CSI)	3429	11.667	2.056	B,C
Waterway Length	1805	28.244	55.215	B,C
Having Waterway	1805	0.299	0.458	B,C
Optimal Route (DEM)	1805	26.861	52.999	B,C
Optimal Route (DEM), Indicator	1805	0.285	0.452	B,C
3. Geographical Control Variables				
Plain	361	0.651	0.477	E
Major river	361	0.488	0.501	E
Coastline	361	0.13	0.337	E
Slope	361	3.077	2.491	E
Elevation	361	5.932	1.558	E
Area	361	9.163	0.332	E
Longitude	361	110.996	5.855	E
Latitude	361	30.692	5.390	E
North China Plain	361	0.207	0.390	E
Northwest China	361	0.127	0.317	E
Upper Yangtze (Sichuan Basin)	361	0.106	0.286	E
Middle Yangtze	361	0.179	0.358	E
Lower Yangtze (Yangtze Delta)	361	0.057	0.218	E
Southeast Coast	361	0.057	0.221	E
Pearl River Basin	361	0.118	0.307	E
Southwest (Yun-Gui Plateau)	361	0.124	0.315	E
4. Agricultural Control Variables				
Suitability of wheat	361	3.969	1.075	F
Suitability of rice	361	2.865	1.126	F
Suitability of maize	361	3.708	1.001	F
Suitability of sweet potato	361	3.833	1.471	F
Suitability of fox millet	361	4.53	1.078	F

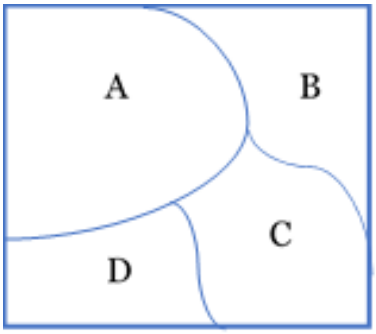
Notes: A: Ge (2000) & Liang (2008); B: Cheng and Xu (1980); C: Galor and Özak (2016); D:China's Military History Editorial Committee (2003); E: CHGIS (2007); F: GAEZ (FAO's Global AgroEcological Zones) (2012)

A.1 Grid-Level Population Density

The raw dataset is the data on prefecture's population (or household number) and area in each sample year. The population data is collected from Ge (2000) and Liang (2008). Since there are only

records of prefecture's household number in Song dynasty, we simulate the prefecture's population by five times the number of households in the year 980, 1080 and 1102. The area of each prefecture is calculated based on the polygon information provided by digital maps. Some prefectures have missing population data, we fill it in with the average population density of neighboring prefectures. We repeat this process until there is no missing population density. Now we have population density and area data for each prefecture. Then we overlay the grid map with the prefecture map in each dynasty and extract the overlapping area of prefectures in each grid. For example, as the following figure shows, the grid i overlaps with four prefectures A, B, C and D. Let the overlapped area of each prefecture be $S_{i,A}$, $S_{i,B}$, $S_{i,C}$, $S_{i,D}$. The population of grid i is the sum of population of each overlapping region, that is $Popu_i = \sum_j S_{i,j} PopDensity_j$. Finally, we divide the grid population ($Popu_i$) by the grid area to get the grid population density.

Figure A.1: Grid's Population



Notes: Illustration of the overlap-area method: grid i overlaps with prefectures A, B, C, and D, and its population is the sum of each prefecture's population density times its overlapping area with grid i.

A.2 Measuring Market Access

A.2.1 Estimating Transportation Cost (τ_{od})

Based on the Historical Maps of China (Cheng and Xu, 1980), we digitalize the maps with waterway and land routes in the Tang, Song, Yuan, Ming and Qing dynasties, and construct transportation networks for each dynasty.

We measure the cost of trade using a simple iceberg cost (τ_{od}). Assuming that varieties produced in grid o and sold in grid o have price $p_{oo}(j)$, and varieties produced in grid o and shipped to grid d for sale have price $p_{od}(j)$, they will satisfy $p_{od}(j) = \tau_{od} p_{oo}(j)$, and $\tau_{od} \geq 1$. Specifically, we calculate our trade cost between origin o and destination d as $\tau_{od} = 1 + RouteCost_{od}$.

$RouteCost_{od}$ is the transport cost for shipping 1 unit variety from origin o to destination d, and $RouteCost_{od} \geq 0$. For the variety produced in grid o and sold in grid o, $RouteCost_{od} = 0$. We calculate $RouteCost_{od}$ by multiplying the baseline route cost rate (per ton-1000 km), with the exact distance traveled.

We take the least transportation cost routes between origin o and destination d to calculate the $RouteCost_{od}$. The routes may include different transportation modes (natural waterways, canal routes, land routes, and trails), and the route cost is the sum of the costs of the different transportation modes included.

(i) Modes of transportation As Figure 2 shows, there are three types of routes, namely natural rivers, canals, and land routes. Moreover, we also need to connect the individual grids to the transportation routes to complete the network. Then, we additionally create the shortest straight-line paths from the centroid of each grid to the nearby waterway or land routes and treat the paths as trail routes. According to the Fogel (1964)'s adjustment factor, the mile traveled is about 1.4 times the shortest straight-line distance. Then, we have four modes of routes. Given the transportation network database, we need to break the routes into segments to permit turns at each intersection, including the intersection of water and land routes, to ensure the connectivity throughout the network. It is worthy to mention that we do not specify where the Grand Canal can switch to other land or natural waterways. In fact, Grand Canal is for tribute grain transportation, and governed by central authority. There are designated trans-shipment warehouses along the canal, such as Suzhou, Huai'an, Yangzhou, Dezhou, Linqing, etc. Grain was transported from various places to transfer warehouses, and then transported along the canal to Beijing by the transport soldiers. So actual canal shipping may be less flexible.

(ii) Trade cost rate parameter for canals Drawing on records from the *Da Ming huidian* (Collected Statutes of the Ming Dynasty) and *Qingdai caoyun* (Grain Transport in the Qing Dynasty) (Li and Jiang, 1995), we set the baseline cost rate parameter for the Grand Canal to 0.249 tons per 1,000 ton-km. This parameter implies that transporting 1 ton of grain over a distance of 1,000 km consumes 0.249 tons of grain in transit. The underlying historical source materials and derivation details are provided below.

We use Suzhou and Yangzhou—two major sources of tribute grain during the Ming and Qing dynasties—as reference points for cost calculations. We focus on the rice consumed during transit, which primarily consists of rations for laborers and animals, and exclude the portion of surplus

rice converted into silver (*yumi zheyin*). We examine the costs associated with *duiyun*, the method of transporting rice to Beijing's warehouses. We find that transport one ton of rice from Suzhou to Beijing (1,500 km) via the Grand Canal incurred an additional 0.4 tons of rice as transit costs. Similarly, shipping one ton from Yangzhou to Beijing (1,300 km) required an extra 0.3 tons. These costs are comparable to those of *gaidui*, an alternative method that delivered rice only to Tongzhou's warehouses rather than Beijing's. Notably, our calculations account solely for in-transit rice consumption.

By construction, the baseline cost parameters based on Suzhou and Yangzhou are 0.267 (0.4/1.5) and 0.231 (0.3/1.3), respectively. We take their average, 0.249 (tons per 1,000 ton-km), as the final baseline cost rate parameter for the Grand Canal.

(iii) Trade cost rate parameter for natural rivers Quan and Kraus (1975), in *Mid-Ching Rice Markets and Trade: An Essay in Price History*, records rice prices across various locations along the Yangtze River from 1723 to 1735. Surplus rice from these locations was shipped to Suzhou, from where it was subsequently transported to Beijing via the Grand Canal under official supervision. Because the book provides both the distances and relative price differentials between Suzhou and each location, we can estimate transportation costs along the Yangtze River using the "price difference method." The relevant historical materials are presented below.

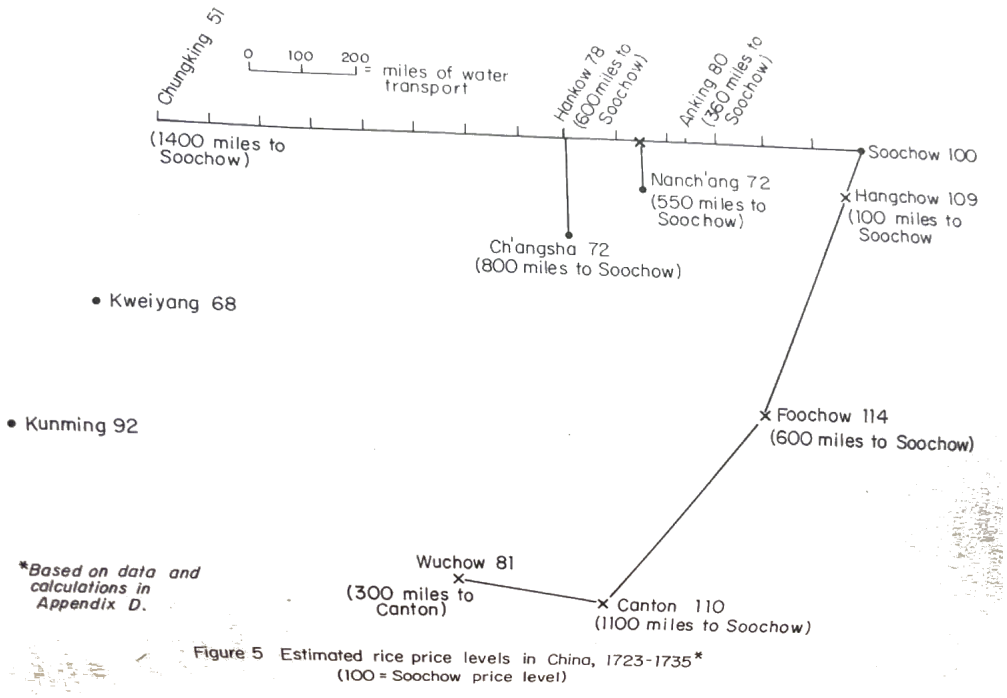
The locations along the Yangtze River shown in this figure include Chongqing, Changsha, Hankou, Nanchang, Anqing, and Suzhou. However, as Quan and Kraus (1975) notes, "the data for Changsha, Hankou and Suzhou are much more dense, internally consistent, and reliable than the data for Nanchang and Anqing." For data accuracy, we exclude Nanchang and Anqing and retain only Chongqing, Changsha, and Hankou for our cost rate calculations.

Specifically, the silver cost rate between an origin o and a destination d is estimated as:

$$SilverCostRate_{od} = \frac{P_d - P_o}{P_o \times Distance_{od}}$$

We calculate the silver cost rate for each city pair among Suzhou, Chongqing, Changsha, and Hankou, yielding an average value of 0.353 per 1,000 ton-km. However, the silver cost rate derived from the price difference method reflects not only the cost of grain in transit, but also additional expenses such as loading and unloading fees, contingent risks, and insurance costs. Because our analysis focuses exclusively on the rice consumed during transit (i.e., the in-transit grain consumption rate), we further refine this estimate. We note that the dataset also contains

Figure A.2.a: Rice Prices along the Yangtze River, 1723–1735



Notes: Reproduced from Quan and Kraus (1975). Prices are used to estimate the natural-waterway transport cost rate via the price-difference method described above.

rice prices for Hangzhou, where grain transportation to Suzhou relied primarily on the Grand Canal. By comparing the silver cost rate of natural waterways with that of canal transport between Suzhou and Hangzhou (0.559 per 1,000 ton-km), we can isolate the in-transit grain cost rate for natural waterways. Consequently, after scaling, the in-transit grain cost rate for natural waterway transportation is $0.249 \times (0.353/0.559) = 0.157$ tons per 1,000 ton-km.

(iv) Trade cost rate parameter for land routes In ancient times, most grain transport relied on four-wheeled or two-wheeled carriages, with the food consumed by humans and animals carried along during transit. Estimating the cost of overland transportation requires information on three key parameters: the daily food consumption of humans and horses, the daily travel distance, and the load capacity. According to *Mengxi bitan* (Dream Pool Essays), a person consumes approximately 0.02 *dan* of rice per day, equivalent to 1.18 kg today. Additionally, Yili Animal Husbandry and Veterinary School of Xinjiang Uygur Autonomous Region (1979) records that a horse under a medium workload requires about 2 kg of grain (typically beans) and 8 kg of fodder per day. Furthermore, a wooden-wheeled carriage carrying a load of 300–450 kg could travel 25–30 km per day on ordinary unpaved or mountainous roads (Zheng et al., 1987). Because these carriage

specifications and road conditions (wooden wheels on dirt roads) closely resemble those of ancient grain transport, we adopt them as a reference and assume that an ancient wooden-wheeled carriage with a 375 kg load could travel 27.5 km per day (taking the midpoint of these ranges).

To assess the efficiency of ancient overland transportation, we propose the following model: consider a 1,000-km journey with post stations or markets every 100 km for resupply. Under this system, carriages need only carry provisions sufficient for 100 km of travel, thereby reducing deadweight load. We examine a horse-drawn carriage with a load capacity of 375 kg that can cover approximately 27.5 km per day on standard dirt roads. The daily consumption rates are 2 kg of grain and 8 kg of fodder for the horse, and 1.18 kg of grain for one human attendant. Thus, transporting goods over 100 km consumes 11.56 kg of grain (human and horse combined) and 29 kg of fodder (horse). After deducting these provisions from the initial payload, 344.44 kg of cargo (375 kg − 11.56 kg − 29 kg) remains for delivery at the 100-km destination. The team then replenishes 11.56 kg of grain and 29 kg of fodder at the local market to continue the journey. According to the *Da Ming huidian* (Collected Statutes of the Ming Dynasty), 1 unit of beans could be exchanged for approximately 5.74 units of fodder during the Jiajing period, providing a historical reference for relative feed costs.

Based on these consumption rates, the total grain expenditure for a 1,000-km one-way journey is $(11.56 + 29/5.74) \times (1,000/100) = 166.12$ kg. Assuming identical consumption for the return trip, the total round-trip expenditure is $166.12 \times 2 = 332.24$ kg of grain. At the same time, the net grain delivered per outward trip remains 344.44 kg. Consequently, the overland transportation cost parameter is calculated as $332.24/344.44 = 0.965$.

Trade cost rate parameter for trails For routes inaccessible to wheeled vehicles, pack animals (such as horses or mules) served as the primary mode of freight transport. Historical records (*Mengxi bitan*) indicate that each pack animal carried 1.5 *dan* (88.8 kg) of grain, traveling at 25 km per day (slower than a wheeled carriage). With daily consumption rates of 1.18 kg of grain for the human attendant and 4 kg of beans for the pack animal (double rations due to the absence of fodder), a 100-km segment (4 days) required 20.72 kg of provisions. A 1,000-km round trip thus consumed 414.4 kg (20.72 kg×10 segments×2), delivering a net payload of only 68.08 kg (88.8 kg−20.72 kg on the outbound journey). This yields a cost ratio parameter of 6.087 (414.4/68.08), meaning that 6.087 kg of grain was expended per 1 kg delivered.

Summary of trade cost rate parameters We summarize the trade cost rate parameters across the four modes of transportation in our model. Water transport includes natural waterways and the Grand Canal, while overland transport comprises mapped roads and manually constructed straight-line trails. Based on historical documents and technical parameters, we set the cost rate for natural waterways at 0.157 tons per 1,000 ton-km, and for the Grand Canal at 0.249 tons per 1,000 ton-km. For overland transport, the cost rate is 0.965 tons per 1,000 ton-km for roads, and 6.087 tons per 1,000 ton-km for trails.

The cost rate of natural waterways is substantially lower than that of the Grand Canal because navigation on natural waterways relied primarily on winds and tides, whereas transport along the Grand Canal depended heavily on human labor (trackers). Similarly, road transport relied on horse-drawn carriages, whereas trail transport was restricted to human porters and pack animals, making trail transport significantly more costly.

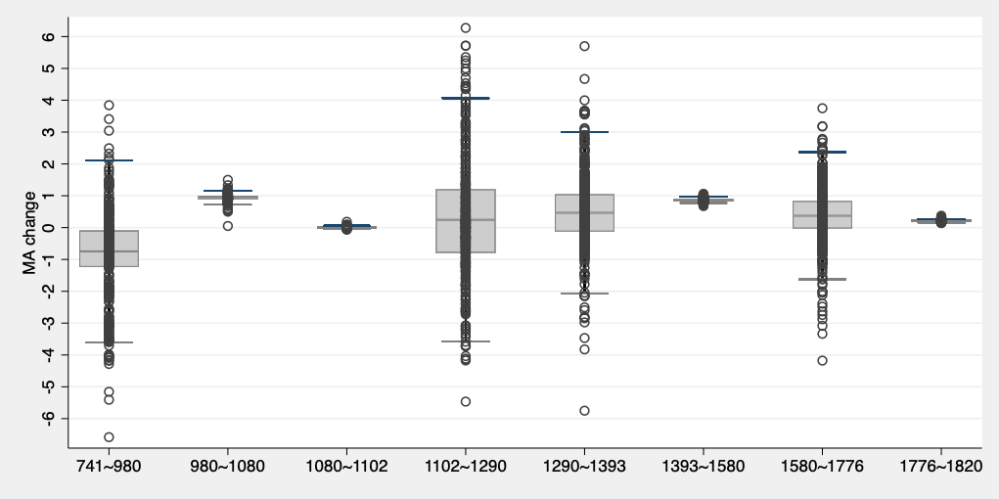
Table A.2: The value of τ

	Route Type	Baseline Route Cost	Alternative Route Cost Assumptions				
			Assump. 1	Assump. 2	Assump. 3	Assump. 4	Assump. 5
1	Natural Waterway	0.157*l	0.157*l	0.157*l	0.157*l	0.157*l	0.353*l
2	Grand Canal	0.249*l	0.249*l	0.249*l	0.249*l	0.249*l	0.559*l
3	Land Routes	0.965*l	0.157*11*l	0.157*5*l	0.157*11*l	0.157*5*l	0.965*(0.559/0.249)*l
4	Trails	6.087*l	0.157*30*l	0.157*30*l	0.249*30*l	0.249*30*l	6.087*(0.559/0.249)*l

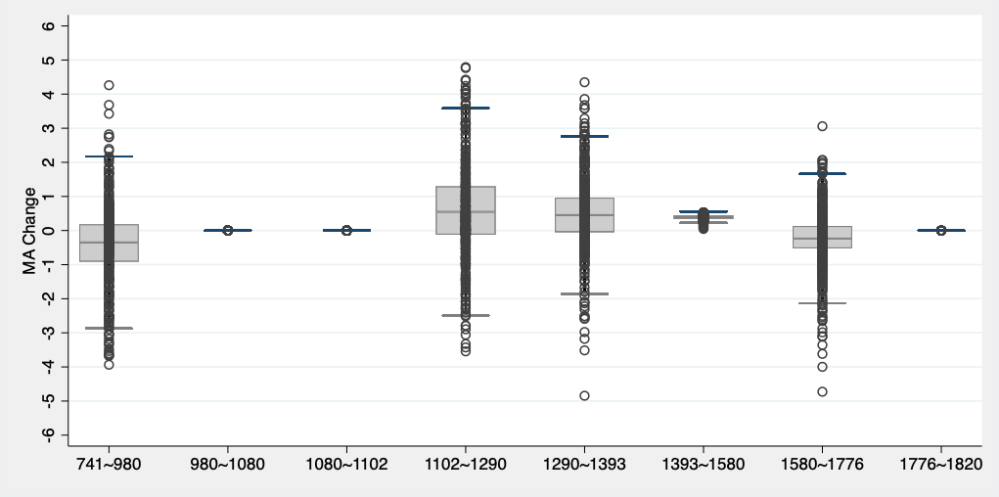
Notes: Baseline and alternative trade-cost rates (tons of grain per 1,000 ton-km) by route type, used to construct τ_{od}. Length (l) in 1000 km.

(vii) Minimum cost route We calculate the minimum transportation cost for every pair of grids by year. We first calculate the least transport cost between two grids along the transportation network using the baseline set of cost rates. But it is unreasonable to directly take this cost as the final minimum cost, because the transport cost along the network may be greater than the cost of a straight-line trail between two grids, especially for adjacent grids that are far away from the transportation network. Hence we estimate the cost of the straight-line trail between two grids, and take the smaller one of the two costs as the final cost. Finally we obtain a transportation cost matrix for each sample year. Applying these cost matrices, we compute market access for each grid in each of our nine sample periods; Figure A.2.b plots the resulting period-to-period changes, which are substantial and reflect two forces, population growth and network change. Holding population fixed at its pre-1500 CSI-based level isolates the network-driven component; by far the largest such change occurs between 1102 and 1290, exactly the Song-Yuan window in which the canal was rerouted.

Figure A.2.b: First Difference of Market Access Shock



(a) Population-based



(b) CSI-based

Notes: Distribution across grids of the period-to-period change in log market access, population-based (a) and CSI-based (b). The upper/lower cap is mean+/- 2 standard deviation. The box is the range of 25%-75%.

Alternative cost rates Additionally, we propose five alternative sets of transport cost rates for robustness checks. Existing historical literature suggests that the cost of standard land roads ranges from 5.5 to 11 times that of transport along the Yangtze River (Quan and Kraus, 1975), while the cost rate of trails can reach up to 30 times that of smooth water transport (Evans, 1984).

Based on these benchmark multiples, we construct four alternative parameter sets.First, we set the cost rates for roads and trails to 11 and 30 times that of natural waterways, yielding 1.727 and 4.710 tons per 1,000 ton-km, respectively. Second, in a minimum scenario, we adopt the lower bound for roads (5.5 times) and 30 times for trails based on natural waterways, resulting in cost rates of 0.864 and 4.710 tons per 1,000 ton-km. Third, in a maximum scenario, we combine the upper bound for roads (11 times natural waterways) with 30 times the cost rate of the Grand Canal for trails, generating rates of 1.727 and 7.470 tons per 1,000 ton-km. Fourth, in an intermediate scenario, we combine 5.5 times natural waterways for roads with 30 times the Grand Canal rate for trails, corresponding to cost rates of 0.864 and 7.470 tons per 1,000 ton-km. Our baseline estimated parameters (0.965 for roads and 6.087 for trails) fall well within the range spanned by these historical alternatives, supporting the reliability of our baseline specification.

As a fifth alternative, we derive a parameter set based directly on the *price difference method*, which naturally incorporates all implicit transport costs. Using historical grain price differentials along the Yangtze River (Quan and Kraus, 1975), we calculate the transport costs for the Grand Canal and natural waterways to be 0.559 and 0.353 tons per 1,000 ton-km, respectively. Due to the scarcity of granular overland price data, we proportionally scale the overland and trail rates to 2.166 and 13.665 tons per 1,000 ton-km.

We confirm the robustness of our main empirical findings across all five alternative specifications in Appendix Tables B.2.b and C.3.a.

Discussion There are several limitations to our transportation cost database. First, the cost rates are held constant across grids and time periods, and do not vary with travel direction. In reality, transportation costs depend heavily on specific local conditions. For instance, water transport costs fluctuate with water flow direction. However, as Donaldson and Hornbeck (2016) argues, maintaining a constant cost rate eliminates potential endogeneity between regional variations in transport costs and local economic development. In this case, temporal changes in market access are driven purely by changes in transportation network infrastructure, which facilitates clean empirical identification. We therefore employ average transport cost rates across the study regions and periods, and demonstrate in robustness checks that our main results hold across alternative cost rate

specifications for both waterway and overland routes.

Second, our baseline measures capture only the grain consumed during transit, omitting other operational costs. In practice, transportation involves storage and inventory expenses for slow-moving shipments, loading and unloading fees, water-land transshipment costs, and maintenance costs for vessels and vehicles. In robustness tests, we show that our baseline findings remain robust when using a comprehensive transportation cost measure derived via the "price difference method."

Third, we model overland transportation using fixed-length segments of 100 km, assuming supply markets are spaced at 100-km intervals along land routes. In actual operations, market intervals may vary. In such cases, transport vehicles must carry additional grain to cover consumption over longer segments, causing local fluctuations in transport costs. To address this, we allow for variations in land transport costs, as detailed in Table A.2.

Appendix B The Optimal Route to the Capital

B.1 Optimal Grand Canal Routes Based on DEM

To address potential endogeneity in historical canal alignments, we construct instrumental variable (IV) routes based on physical topography using Digital Elevation Models (DEMs).

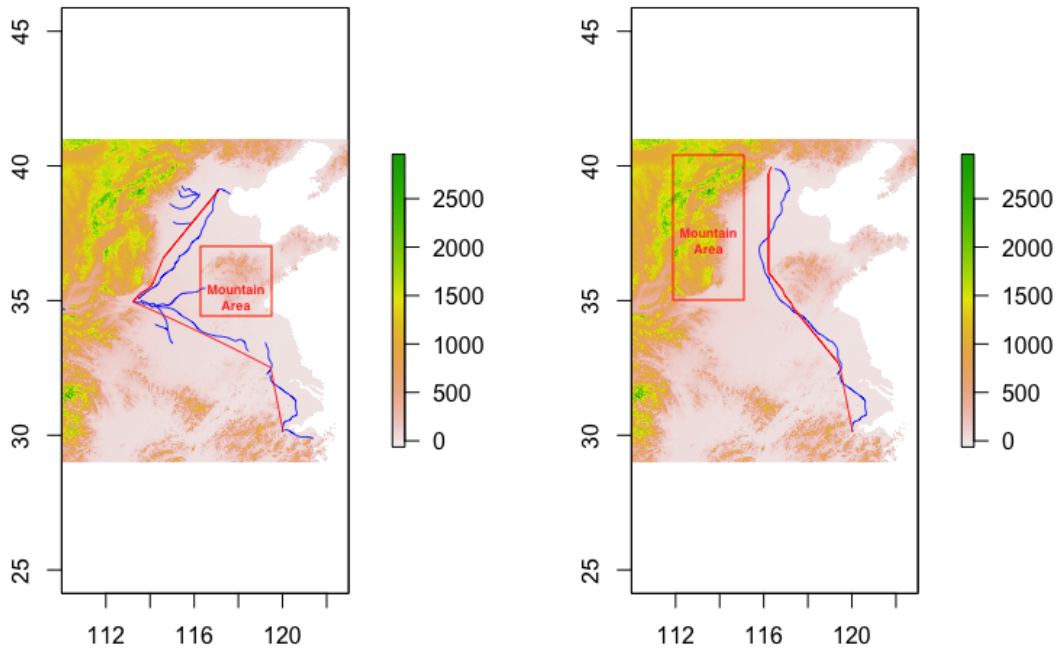
During the Tang and Song dynasties, the eastern slope of the Taihang Mountains constrained the trajectory of the Beijing–Kaifeng section of the Grand Canal. To construct an exogenous hypothetical route, we utilize a 500 m $\times$ 500 m resolution DEM map to identify the maximum elevation encountered along the actual canal route (196 m). We then exclude all grid cells exceeding 196 m in elevation and compute the shortest feasible path (least-cost path) across the remaining terrain for the Beijing–Kaifeng segment.

For the Kaifeng–Yangzhou segment, where the maximum elevation along a direct line remains well below 196 m, we employ the hypothetical straight-line route as the IV trajectory. Figure B.1 illustrates the optimal canal routes in the Song Dynasty (red lines) alongside the actual historical alignment (blue lines).

For the Yuan, Ming, and Qing Dynasties (post-1290), the canal was re-routed directly to connect Beijing and Yangzhou, bypassing the central Shandong Massif. To generate the corresponding IV route for the Beijing–Yangzhou corridor, we construct the shortest path constrained by the elevation threshold of the Shandong mountains. Specifically, we identify the maximum elevation along the

actual canal segment passing through Shandong (95 m), mask out areas in Shandong exceeding this threshold, and calculate the shortest path through the remaining terrain. Taking the Ming Dynasty as a representative example, Figure B.1 displays the topography-based optimal canal routes (red lines) against the actual Grand Canal course (blue lines).

Figure B.1: Constructing Optimal Routes to the National Capital



Notes: The blue lines are the actual Grand Canal, the red lines are optimal canal route (based on DEM).

B.2 Robustness of Market Access Based on the Optimal Route

We next check the robustness of the relationship between market access based on the optimal route and actual market access (Table 1, Panel B, in the main text) to two choices: the value of the trade elasticity θ and the transportation cost parameters.

In Table B.2.a, we set different values of θ for market access taken by other empirical researches as mentioned in Section 2.2, while hold the transportation costs for each route type unchanged. While Table B.2.b adopt alternative cost parameters in Table A.2, as described in Appendix A.2.1, and keep the value of θ at 8.62.

Table B.2.a: Market Access Based on Optimal Route: Theta Changes

Dependent variable	ln MA (Baseline Route Cost, Alt. θ values)											
	(1)	(2)	(3)	(4)	(5)	(6)	(7)	(8)	(9)	(10)	(11)	(12)
	θ= 1		θ= 3.6		θ= 8.22		θ= 8.08		θ= 9.04		θ= 12.86	
ln MA (optimal, pre-1500 CSI)	0.508***		0.510***		0.513***		0.513***		0.513***		0.511***	
	(0.042)		(0.042)		(0.048)		(0.048)		(0.049)		(0.050)	
ln MA (optimal, Tang popu.)		0.485***		0.498***		0.534***		0.534***		0.533***		0.523***
		(0.038)		(0.038)		(0.041)		(0.041)		(0.041)		(0.043)
Grid FE	Y	Y	Y	Y	Y	Y	Y	Y	Y	Y	Y	Y
Year FE	Y	Y	Y	Y	Y	Y	Y	Y	Y	Y	Y	Y
GeoControl × Year FE	Y	Y	Y	Y	Y	Y	Y	Y	Y	Y	Y	Y
AgriControl × Year FE	Y	Y	Y	Y	Y	Y	Y	Y	Y	Y	Y	Y
R-squared	0.990	0.990	0.949	0.950	0.908	0.913	0.909	0.914	0.904	0.910	0.893	0.898
Observations	3,249	3,249	3,249	3,249	3,249	3,249	3,249	3,249	3,249	3,249	3,249	3,249

Notes: Columns vary the trade elasticity $\theta \in \{1, 3.6, 8.22, 8.08, 9.04, 12.86\}$, holding baseline route costs fixed, using the CSI-weighted (odd columns) or Tang-population-weighted (even columns) instrument. Control variables are the same as those listed in Table 1. Standard errors displayed in parentheses are clustered at grid level. *** $p < 0.01$, ** $p < 0.05$, * $p < 0.1$.

Table B.2.b: Market Access Based on Optimal Route: Alternative Route Costs

Dependent variable	ln MA (θ= 8.62, Alt. Route Cost Assumps.)									
	(1)	(2)	(3)	(4)	(5)	(6)	(7)	(8)	(9)	(10)
	Assump. 1		Assump. 2		Assump. 3		Assump. 4		Assump. 5	
ln MA (optimal, pre-1500 CSI)	0.661***		0.527***		0.576***		0.480***		0.515***	
	(0.044)		(0.049)		(0.045)		(0.050)		(0.049)	
ln MA (optimal, Tang popu.)		0.647***		0.545***		0.582***		0.506***		0.524***
		(0.034)		(0.040)		(0.038)		(0.043)		(0.044)
Grid FE	Y	Y	Y	Y	Y	Y	Y	Y	Y	Y
Year FE	Y	Y	Y	Y	Y	Y	Y	Y	Y	Y
GeoControl × Year FE	Y	Y	Y	Y	Y	Y	Y	Y	Y	Y
AgriControl × Year FE	Y	Y	Y	Y	Y	Y	Y	Y	Y	Y
R-squared	0.942	0.946	0.917	0.922	0.918	0.924	0.891	0.896	0.897	0.900
Observations	3,249	3,249	3,249	3,249	3,249	3,249	3,249	3,249	3,249	3,249

Notes: Columns vary the route-cost assumption (Assumptions 1–5, Appendix A.2.1) at $\theta = 8.62$, using the CSI-weighted (odd columns) or Tang-population-weighted (even columns) instrument. Control variables are the same as those listed in Table 1. Standard errors displayed in parentheses are clustered at grid level. *** $p < 0.01$, ** $p < 0.05$, * $p < 0.1$.

B.3 Placebo Tests: Song vs. Yuan Optimal Routes

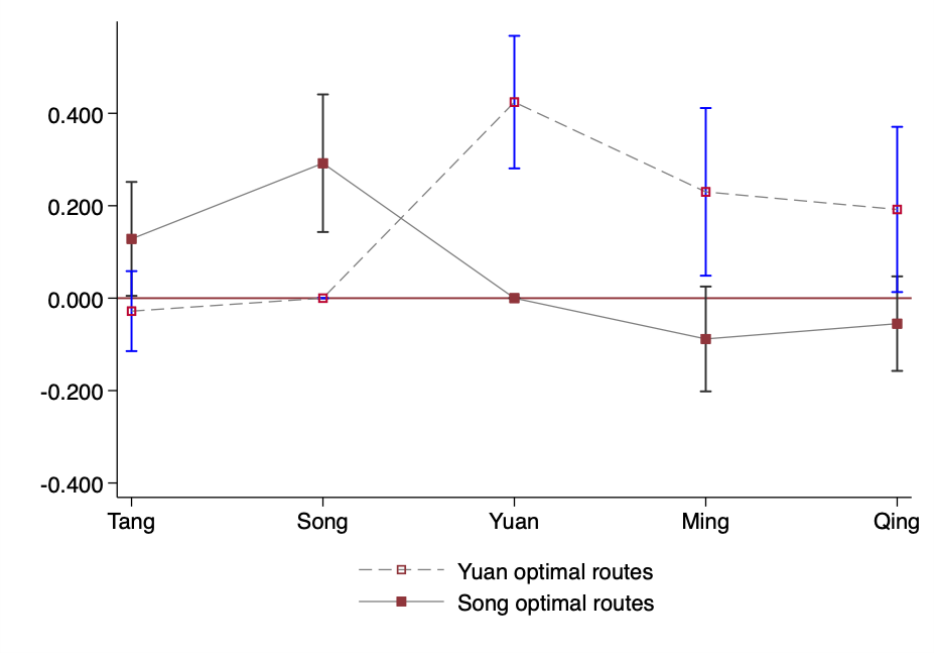
The most striking change in the waterway occurred during the Song-Yuan transition, when the national capital moved from the central plain to Beijing in the north. We define two additional optimal routes fixed across all five dynasties, one to the Song capital ($OptimalRoute_{i,Song}$) and one to the Yuan capital ($OptimalRoute_{i,Yuan}$), using the same DEM-based procedure as in Appendix

B.1, and examine each route's predictive power on the actual waterway dynasty by dynasty:

$$Waterway_{id} = \sum_{d=1}^{d=5}(OptimalRoute_{i,Song/Yuan} \times I_{\rho=d})\alpha^{\rho} + \sum_{d=1}^{d=5}(Z_i \times I_{\rho=d})\gamma^{\rho} + \lambda_i + \eta_d + \epsilon_{id} \tag{7}$$

where $Waterway_{id}$ is the actual waterway in grid i and dynasty d; Z_i is the set of time-invariant geographic and agricultural controls described in Section 2.2; and λ_i and η_d are grid and dynasty fixed effects, with standard errors clustered at the grid level. We estimate this specification separately for the Song and the Yuan optimal routes and plot the resulting dynasty-specific coefficients α^{ρ} in Figure B.3.

Figure B.3: Effects of Song-Yuan Optimal Routes to the National Capital



Notes: The solid line represents the effect of Song optimal routes on the actual waterway by dynasty, while the dashed line represents the effect of Yuan optimal routes. Bars denote 95% confidence intervals based on standard errors clustered at the grid level.

As Figure B.3 shows, the predictive power of the optimal route to the Song capital declines exactly when the national capital moves from the central plain to Beijing. The optimal route to Beijing shows the mirror-image pattern: it predicts the actual waterway well from the Yuan dynasty onward, but not during the Tang or Song. In other words, grids along the optimal route to the Song capital become less likely to have a waterway once the capital relocates to Beijing, while grids

along the optimal route to the Yuan capital become more likely to have one, precisely from the point of relocation onward.

Appendix C Market Access and Population Density

C.1 Exclusion Restriction

As discussed in Section 4.1, a threat to our IV strategy is that the optimal route to the capital could predict direct, place-based state investment rather than working solely through market access. Because such investment should raise population locally, in grids on or beside the route, rather than through a grid's broader access to distant markets, we address this concern by restricting market access, for both the endogenous regressor and the instrument, to grids beyond the immediate neighborhood.

We progressively exclude first-order neighboring grids (within approximately 100 km) and second-order neighboring grids (within approximately 200 km) from the market access calculation, reconstructing both the actual market access regressor and the optimal-route-based instrument this way. The results suggest that market access to more distant regions still significantly contributes to local population growth, for both the OLS and IV specifications. Table C.1 presents the results.

Table C.1: Market Access beyond Neighbor Grids

Dependent variable	ln Popu. Density							
	(1)	(2)	(3)	(4)	(5)	(6)	(7)	(8)
	OLS				IV: ln MA (excl. nbr grids, opt., pre-1500 CSI)		IV: ln MA (excl. nbr grids, opt., Tang popu.)	
ln MA (excl. 1st nbr)	0.086***		0.099***		0.207***		0.230***	
	(0.023)		(0.017)		(0.041)		(0.041)	
ln MA (excl. 1st& 2nd nbr)		0.041*		0.086***		0.232***		0.230***
		(0.023)		(0.017)		(0.040)		(0.040)
Grid FE	Y	Y	Y	Y	Y	Y	Y	Y
Year FE	Y	Y	Y	Y	Y	Y	Y	Y
GeoControl × Year FE			Y	Y	Y	Y	Y	Y
AgriControl × Year FE			Y	Y	Y	Y	Y	Y
KP F-stat					127.66	148.54	135.06	145.78
R-squared	0.794	0.791	0.888	0.888	-0.005	-0.041	-0.021	-0.039
Observations	3,249	3,249	3,249	3,249	3,249	3,249	3,249	3,249

Notes: ln MA (excl. 1st nbr) measures market access excluding first-order neighboring grids (within approximately 100 km); *ln MA (excl. 1st & 2nd nbr)* further excludes second-order neighboring grids (within approximately 200 km). Control variables are the same as those listed in Table 1. Standard errors displayed in parentheses are clustered at grid level. *** $p < 0.01$, ** $p < 0.05$, * $p < 0.1$.

C.2 Shock in Market Access: An Event-study Approach

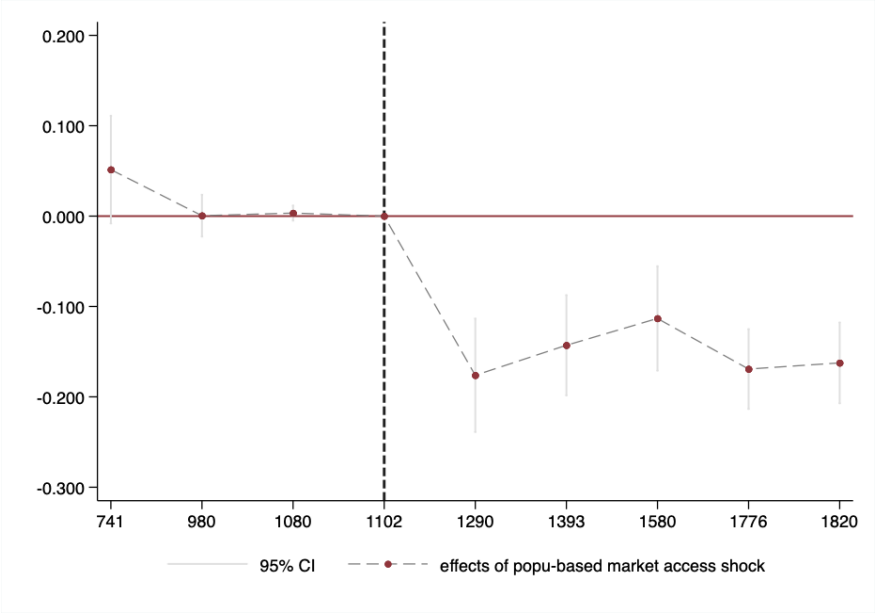
To what extent the population density is affected by the sudden change of market access caused by the shortening of the Grand Canal after Song Dynasty? To answer this question, we first define "market access shock" as actual market access in 1102 minus that in 1290. Theoretically, the shock should only have impact on the population density after the Song Dynasty. To examine the parallel trends in the effects, we interact the market access shock with a full set of period dummies, and display the estimated coefficients of market access shock in each sample year in Figure C.2a. The impact of market access shock does not show a clear pre-trend before 1102, and suddenly becomes negatively significant in 1290 with a magnitude of 0.176. The impact then rebounds to -0.143 in1393 and keeps between -0.2 and -0.1 in the subsequent sample years, indicating the impact is permanent.

Market access shocks may come from two sources, one is the shortening of the Grand Canal, which is of our interest; the other is endogenous demographic changes related to wars, trade costs and in local political status. To extract the part of impact caused by the rerouting of the Grand Canal, we use the pre-1500 CSI to represent the population in the construction of the market access shock from 1102 to 1290. The annual impact of CSI-based market access shock is shown in Figure C.2b. The trend of the impact is similar to that in Figure C.2a, reflecting a permanent negative effect of the shortening canal on population density through changing market access.

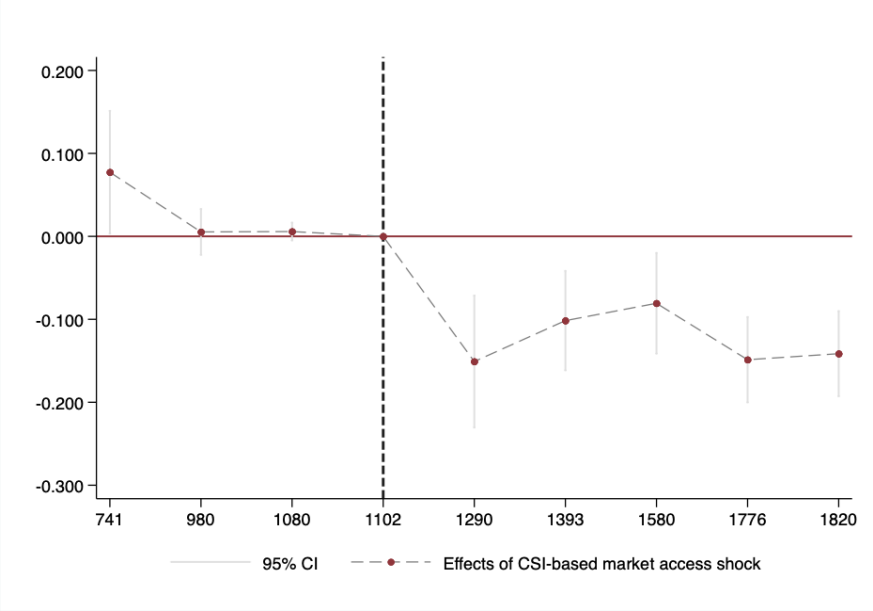
C.3 Additional Checks

(i) Varying parameters Table C.3.a shows the result is robustness to market access with different values of θ (the "trade elasticity") and alternative transportation cost settings. In columns (1) to (6), we set different values of θ for market access taken by other empirical researches as mentioned in Section 2.2, while hold the transportation costs for each route type unchanged. Columns (7) to (11) adopt alternative cost parameters in Table A.2, and keep the value of θ at 8.62.

Figure C.2: Dynamic Effects of Song-Yuan Market Access Shock



(a) Population-based market access shock



(b) CSI-based market access shock

Notes: The solid line represents the effect of Song-Yuan market access shock on population density.

Table C.3.a: Impact of Market Access on Population Density: Changing Parameters

Dependent variable	ln Popu. Density										
	(1)	(2)	(3)	(4)	(5)	(6)	(7)	(8)	(9)	(10)	(11)
Panel A	Alt. θ values (Baseline Route Cost)						Alt. Route Cost Assumps. (θ= 8.62)				
	θ= 1	θ= 3.6	θ= 8.22	θ= 8.08	θ= 9.04	θ=12.86	Assump. 1	Assump. 2	Assump. 3	Assump. 4	Assump. 5
ln MA	0.841***	0.269***	0.148***	0.150***	0.139***	0.109***	0.215***	0.173***	0.145***	0.116***	0.109***
	(0.164)	(0.043)	(0.019)	(0.019)	(0.017)	(0.013)	(0.023)	(0.021)	(0.017)	(0.016)	(0.013)
Grid FE	Y	Y	Y	Y	Y	Y	Y	Y	Y	Y	Y
Year FE	Y	Y	Y	Y	Y	Y	Y	Y	Y	Y	Y
GeoControl × Year FE	Y	Y	Y	Y	Y	Y	Y	Y	Y	Y	Y
AgriControl × Year FE	Y	Y	Y	Y	Y	Y	Y	Y	Y	Y	Y
R-squared	0.888	0.889	0.891	0.891	0.891	0.891	0.893	0.891	0.892	0.890	0.891
Observations	3,249	3,249	3,249	3,249	3,249	3,249	3,249	3,249	3,249	3,249	3,249
Panel B											
ln MA (Std.)	0.228***	0.263***	0.306***	0.305***	0.308***	0.312***	0.432***	0.332***	0.345***	0.271***	0.307***
	(0.043)	(0.042)	(0.040)	(0.040)	(0.039)	(0.037)	(0.047)	(0.042)	(0.041)	(0.038)	(0.037)
Grid FE	Y	Y	Y	Y	Y	Y	Y	Y	Y	Y	Y
Year FE	Y	Y	Y	Y	Y	Y	Y	Y	Y	Y	Y
GeoControl × Year FE	Y	Y	Y	Y	Y	Y	Y	Y	Y	Y	Y
AgriControl × Year FE	Y	Y	Y	Y	Y	Y	Y	Y	Y	Y	Y
R-squared	0.888	0.888	0.890	0.890	0.891	0.891	0.893	0.891	0.891	0.890	0.891
Observations	3,249	3,249	3,249	3,249	3,249	3,249	3,249	3,249	3,249	3,249	3,249

Notes: Panel A varies θ (columns (1)-(6)) or the route-cost assumption (columns (7)-(11), Appendix A.2.1); Panel B repeats these specifications with ln MA standardized. Control variables are the same as those listed in Table 1. Standard errors displayed in parentheses are clustered at grid level. *** $p < 0.01$, ** $p < 0.05$, * $p < 0.1$.

(ii) CSI Based Market Access Baseline market access is based on the population in each grid. For robustness and to mitigate the endogeneity to the grid population, we use the Caloric Suitability Index (CSI) provided by Galor and Özak (2016), to indicate the population that the grid can support, denoted by $MA_{i,t} = \sum_{d \neq i} \tau_{id,t}^{-\theta} CSI_{d,t}$. Table C.3.b shows that CSI-based market access has a significantly positive effect on population density.

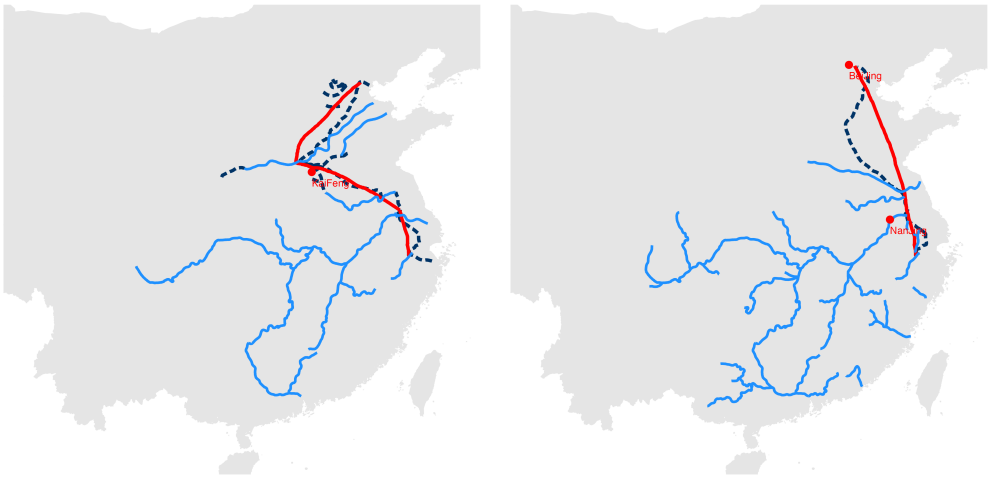
Table C.3.b: The Impact of CSI-based Market Access

Dependent variable	ln Popu. Density			
	OLS		2SLS	
	(1)	(2)	(3)	(4)
			IV:ln MA (optimal, pre-1500 CSI)	IV:ln MA (optimal, Tang popu.)
ln MA (raw route, CSI-based)	0.109***	0.111***	0.176***	0.292***
	(0.025)	(0.021)	(0.053)	(0.058)
Grid FE	Y	Y	Y	Y
Year FE	Y	Y	Y	Y
GeoControl × Year FE		Y	Y	Y
AgriControl × Year FE		Y	Y	Y
KP F-stat			113.44	137.25
R-squared	0.794	0.888	0.014	-0.037
Observations	3,249	3,249	3,249	3,249

Notes: ln MA (raw, CSI-based) uses the Caloric Suitability Index in place of population; war-shock controls as in Table C.3.d. Control variables are the same as those listed in Table 1. Standard errors displayed in parentheses are clustered at grid level. *** $p < 0.01$, ** $p < 0.05$, * $p < 0.1$.

(iii) Alternative optimal route to national capital We define different type of optimal route to construct the instrumental variable to check the robustness of the results. We first obtain the canal route with the least travel time by introducing the Human Mobility Index (HMI) provided by Özak (2018). Specifically, HMI estimates potential minimum travel times (in hours) around the world, taking into account human biological limitations, as well as the geographic and technological factors that determined travel times before the widespread use of steam power (Figure C.3.a). Second, we directly take the shortest straight-line (STL) path connecting major locations as an approximation of the Grand Canal, without considering elevation issues (Figure C.3.b). Although these optimal routes are not as precise as the baseline optimal routes shown in Appendix Figure B.1, they can predict the actual canal routes to a certain extent. Table C.3.c shows the IV estimations of these two instrumental variables with alternative optimal canal routes.

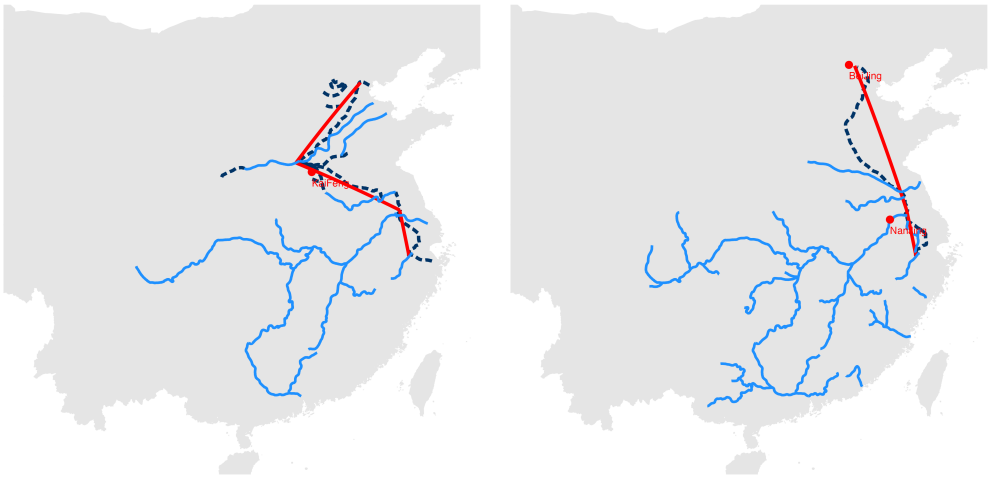
Figure C.3.a: Optimal Routes to the National Capital (Human Mobility Index)



(a) Song **(b)** Ming

Notes: The blue lines are waterways, the dashed lines are the actual Grand Canal, the red lines are optimal routes to national capital. The red points are national capitals in each dynasty.

Figure C.3.b: Optimal Routes to the National Capital (Shortest Straight-Line)



(a) Song **(b)** Ming

Notes: The blue lines are waterways, the dashed lines are the actual Grand Canal, the red lines are optimal routes to national capital. The red points are national capitals in each dynasty.

Table C.3.c: IV Based on Alternative Definition of Optimal Route

Panel A: 2SLS	ln Popu. Density			
	(1)	(2)	(3)	(4)
	IV: ln MA (HMI-opt., pre-1500 CSI)	IV: ln MA (HMI-opt., Tang popu.)	IV: ln MA (STL-opt., pre-1500 CSI)	IV: ln MA (STL-opt., Tang popu.)
ln MA	0.187***	0.256***	0.193***	0.262***
	(0.054)	(0.050)	(0.053)	(0.050)
Grid FE	Y	Y	Y	Y
Year FE	Y	Y	Y	Y
GeoControl × Year FE	Y	Y	Y	Y
AgriControl × Year FE	Y	Y	Y	Y
KP F-stat	59.46	83.42	66.97	95.87
R-squared	0.045	0.019	0.044	0.016
Observations	3,249	3,249	3,249	3,249
Panel B: First-stage	ln MA			
	(1)	(2)	(3)	(4)
ln MA (HMI-opt., pre-1500 CSI)	0.429***			
	(0.056)			
ln MA (HMI-opt., Tang popu.)		0.477***		
		(0.052)		
ln MA (STL-opt., pre-1500 CSI)			0.437***	
			(0.053)	
ln MA (STL-opt., Tang popu.)				0.475***
				(0.049)
Grid FE	Y	Y	Y	Y
Year FE	Y	Y	Y	Y
GeoControl × Year FE	Y	Y	Y	Y
AgriControl × Year FE	Y	Y	Y	Y
R-squared	0.903	0.908	0.903	0.908
Observations	3,249	3,249	3,249	3,249

Notes: Panel A reports 2SLS estimates and Panel B the corresponding first stage; columns (1)-(2) instrument with the Human-Mobility-Index-based optimal route and columns (3)-(4) with the shortest-straight-line-based optimal route (Appendix Figures C.3.a–C.3.b). Control variables are the same as those listed in Table 1. Standard errors displayed in parentheses are clustered at grid level. *** $p < 0.01$, ** $p < 0.05$, * $p < 0.1$.

(iv) The impact of Sino-nomadic war The determination on shortening the Grand Canal may depends on two historical events. The first one is the relocation of the national capital from Kaifeng

to Beijing from the Yuan Dynasty. The Grand Canal is aimed at transporting tribute grains to northern national capital, it is not necessary to go through the Central Plains as the political center shifted to Beijing. Second, frequent wars occurred before the founding of the Yuan Dynasty: Jin troops captured Kaifeng in 1127, ending the Northern Song, and the Mongols, after subduing the Jin by 1234, went on to extinguish the Southern Song in 1279 at a cost of some 35–40 million lives, which led to a sharp decline in the population of the Central Plains. Therefore, it is not valuable to build a canal through the Central Plains. In this section we focus on the wars between 1211 and 1279 CE, which can change market access and population density by reducing the population. We measure the warfare in terms of the number of wars occurred in each grid during 1211-1279, and the number of deaths measured by the difference in the logarithm of population between the year 1102 and 1290.

Table C.3.d reports the results incorporating these historical warfare controls. Column (2) indicates that conflict-induced population loss exerts a strong negative impact on subsequent population density, whereas war frequency alone yields no statistically significant effect. Importantly, after absorbing the confounding effects of warfare shocks, the estimated effect of market access remains substantial—declining modestly from 0.143 (column 1) to 0.096 (column 2). The IV estimates yield virtually identical conclusions.

Table C.3.d: The Role of Sino-nomadic War

Dependent variable	ln Popu. Density					
	(1)	(2)	(3)	(4)	(5)	(6)
	OLS		IV: ln MA (optimal, pre-1500 CSI)		IV: ln MA (optimal, Tang popu.)	
ln MA	0.143***	0.096***	0.159***	0.133***	0.239***	0.187***
	(0.018)	(0.018)	(0.045)	(0.042)	(0.043)	(0.041)
post1290 × number of wars		0.008		0.007		0.006
		(0.019)		(0.019)		(0.019)
post1290 × number of deaths		-0.214***		-0.204***		-0.187***
		(0.036)		(0.036)		(0.035)
Grid FE	Y	Y	Y	Y	Y	Y
Year FE	Y	Y	Y	Y	Y	Y
GeoControl × Year FE	Y	Y	Y	Y	Y	Y
AgriControl × Dynasty FE	Y	Y	Y	Y	Y	Y
KP F-stat			110.67	119.71	170.78	165.35
R-squared	0.891	0.900	0.049	0.123	0.028	0.108
Observations	3,249	3,249	3,249	3,249	3,249	3,249

Notes: post1290 × number of wars and post1290 × number of deaths measure, respectively, the count of Sino-nomadic wars in each grid during 1211–1279 and the resulting log population decline between 1102 and 1290, interacted with a post-1290 indicator. Control variables are the same as those listed in Table 1. Standard errors displayed in parentheses are clustered at grid level. *** $p < 0.01$, ** $p < 0.05$, * $p < 0.1$.

(v) The role of provincial capitals We also explore whether the political status of provincial capital can affect the local market access by improving regional transportation network, and thereby increasing local population density. We follow Bai and Jia (2023) and include the dummy variable indicating whether a provincial capital is located in the grid. The results in Table C.3.e demonstrate that, being a provincial capital can significantly increase local population density by approximately 27% (column 2), but cannot effectively explain the positive impact of market access on population density. This shows that provincial capital status has limited effect on the development of local transportation network, including the new route of the Grand Canal.

Table C.3.e: The Role of Provincial Capital

Dependent variable	ln Popu. Density			
	(1)	(2)	(3)	(4)
	OLS		IV: ln MA (optimal, pre-1500 CSI)	IV: ln MA (optimal, Tang popu.)
ln MA	0.200***	0.173***	0.116**	0.181***
	(0.026)	(0.024)	(0.048)	(0.044)
Prov.Capital	0.177***	0.270***	0.289***	0.267***
	(0.061)	(0.059)	(0.067)	(0.064)
Grid FE	Y	Y	Y	Y
Year FE	Y	Y	Y	Y
GeoControl × Year FE		Y	Y	Y
AgriControl × Year FE		Y	Y	Y
KP F-stat			84.40	130.96
R-squared	0.855	0.919	0.119	0.128
Observations	2,527	2,527	2,527	2,527

Notes: Prov. Capital is an indicator for whether a provincial capital is located in the grid (Bai and Jia, 2023); Control variables are the same as those listed in Table 1. Standard errors displayed in parentheses are clustered at grid level. *** $p < 0.01$, ** $p < 0.05$, * $p < 0.1$.

(vi) Selection of land routes We further address potential concerns regarding the endogenous selection of land routes, which could generate a spurious relationship between population density and market access. While route selection is partially driven by exogenous factors—such as political considerations, topography, and node connections to major cities—it may also be biased toward more prosperous areas. To isolate this, we examine changes in market access orthogonal to local transportation infrastructure by controlling for route length in and around each grid. Table C.3.f presents the results: column (1) controls for route length within each grid, while columns (2) and (3) sequentially incorporate controls for route lengths in first- and second-order neighboring grids.

Table C.3.f: Control for Length of Land Routes

Dependent variable	ln Popu. Density								
	(1)	(2)	(3)	(4)	(5)	(6)	(7)	(8)	(9)
	OLS			IV: ln MA (optimal, pre-1500 CSI)			IV: ln MA (optimal, Tang popu.)		
ln MA	0.140***	0.125***	0.115***	0.160***	0.156***	0.153***	0.244***	0.241***	0.235***
	(0.020)	(0.021)	(0.022)	(0.049)	(0.049)	(0.050)	(0.045)	(0.047)	(0.048)
Grid FE	Y	Y	Y	Y	Y	Y	Y	Y	Y
Year FE	Y	Y	Y	Y	Y	Y	Y	Y	Y
GeoControl × Year FE	Y	Y	Y	Y	Y	Y	Y	Y	Y
AgriControl × Year FE	Y	Y	Y	Y	Y	Y	Y	Y	Y
Landroute Length (grid)	Y	Y	Y	Y	Y	Y	Y	Y	Y
Landroute Length(nbr)		Y	Y		Y	Y		Y	Y
Landroute Length(nbr2)			Y			Y			Y
KP F-stat				123.71	127.86	128.94	181.84	188.39	188.34
R-squared	0.891	0.892	0.893	0.049	0.055	0.062	0.030	0.033	0.041
Observations	3,249	3,249	3,249	3,249	3,249	3,249	3,249	3,249	3,249

Notes: Land Route Length (grid) is the length of land route across the grid. *Land Route Length (nbr)* is the length of land route across the neighbor grids. *Land Route Length (nbr2)* is the length of land route across the neighbor's neighbor grids. Control variables are the same as those listed in Table 1. Standard errors displayed in parentheses are clustered at grid level. *** $p < 0.01$, ** $p < 0.05$, * $p < 0.1$.

Appendix D Model and Counterfactual Analysis

D.1 Model

Model setup This section provides a detailed discussion of the model. The framework is based on Eaton and Kortum (2002) and Donaldson and Hornbeck (2016). The basic setup is a trade model as in Eaton and Kortum (2002) with the immobile production factor land and the mobile factors labor and capital. The economy consists of many trading regions (grids), where the origin of a trade is indexed by o and the destination by d.

Consumers have CES preferences over a continuum of differentiated goods indexed by j, and the indirect utility of a consumer with income y_o and facing prices P_o is,

$$V(P_o, y_o) = \frac{y_o}{P_o} \tag{A1}$$

where P_o is a CES price index of the form $P_o = \left(\int_j p_o(j)^{1-\sigma} dj\right)^{\frac{1}{1-\sigma}}$. Each district produces varieties with a Cobb-Douglas technology using land (T), labor (L), and capital (K),

$$x_o(j) = z_o(j)(T_o(j))^{\alpha}(L_o(j))^{\gamma}(K_o(j))^{1-\alpha-\gamma} \tag{A2}$$

The production function implies the marginal cost is

$$MC_o(j) = \frac{q_o^{\alpha} w_o^{\gamma} r_o^{1-\alpha-\gamma}}{z_o(j)} \tag{A3}$$

where q_o is the land rental rate, w_o is the wage, and r_o is the interest rate. Following Eaton and Kortum (2002), $z_o(j)$ is an exogenous productivity shifter drawn from a Fréchet distribution with CDF $F_o(z) = \Pr[Z_o \leq z] = \exp(-A_o z^{-\theta})$, where $\theta > 1$ captures the standard deviation of productivity, corresponding to the scope of comparative advantage, and A_o is a grid's state of absolute technology advantage. Following Donaldson and Hornbeck (2016), we assume the capital is perfectly mobile so that the return to capital is equalized across all grids in the same period (i.e., $r_o = r$).

Trade costs between locations o and d are modeled based on "iceberg" cost. For one unit of a good to reach destination d, $\tau_{od} \geq 1$ units must be shipped from origin o. This implies that if a good is produced in location o and sold at the price $p_{oo}(j)$, then it is sold in location d at the price $p_{od}(j) = \tau_{od} p_{oo}(j)$. Due to perfect competition, prices equal the marginal costs of producing each variety.

Eaton and Kortum (2002) derive two important results for our model. The first is that the consumer price index in destination location d takes the form[6]

$$P_d^{-\theta} = \kappa_1 \sum_o [A_o (\tau_{od} q_o^{\alpha} w_o^{\gamma})^{-\theta}] \equiv CMA_d \tag{A4}$$

We follow Donaldson and Hornbeck (2016) in referring to this price index as CMA_d (Consumer Market Access); it measures district d's access to cheap goods (i.e., low production costs in supplying district and low trade costs).

The second important result drawn from Eaton and Kortum (2002) describes the value of total export X_{od} from o to d, as

$$X_{od} = \kappa_1 A_o (q_o^{\alpha} w_o^{\gamma})^{-\theta} (\tau_{od})^{-\theta} P_d^{\theta} Y_d \tag{A5}$$

[6]Here, κ_1 is a constant defined by $\kappa_1 \equiv \left[\Gamma\left(\frac{\theta+1-\sigma}{\theta}\right)\right]^{-\frac{\theta}{1-\sigma}} r^{-(1-\alpha-\gamma)\theta}$, where $\Gamma(\cdot)$ is the Γ function defined by $\Gamma(t) = \int_0^{\infty} x^{t-1} e^{-x} dx$ (Donaldson and Hornbeck, 2016).

which can also be written as

$$X_{od} = \kappa_1 A_o (q_o^{\alpha} w_o^{\gamma})^{-\theta} Y_d CMA_d^{-1} \tau_{od}^{-\theta} \tag{A6}$$

Solving the model Equation (A6) is a gravity equation with the standard features that trade increases in income of the destination and in productivity of the origin, while trade decreases in production costs, trade costs, and in consumer market access of the destination. Summing the gravity equation over destinations d and assuming that goods markets clear yields total income of origin o,

$$Y_o = \sum_d X_{od} = \kappa_1 A_o (q_o^{\alpha} w_o^{\gamma})^{-\theta} \sum_d [\tau_{od}^{-\theta} CMA_d^{-1} Y_d] \tag{A7}$$

Donaldson and Hornbeck define "firm market access" of district o as

$$FMA_o \equiv \sum_d \tau_{od}^{-\theta} CMA_d^{-1} Y_d \tag{A8}$$

Using Equations (A7) and (A8) into the definition of CMA_d in Equation (A4) yields that

$$CMA_d = \sum_o \tau_{od}^{-\theta} FMA_o^{-1} Y_o \tag{A9}$$

Following Donaldson and Hornbeck (2016), if trade costs are symmetric, the solution to Equations (A8) and (A9) must satisfy $FMA_o = \rho CMA_o = MA_o$ for $\rho > 0$ and they refer to MA_o as "market access" in district o. Therefore, we get

$$MA_o = \rho \sum_d \tau_{od}^{-\theta} MA_d^{-1} Y_d \tag{A10}$$

We also derive the relationship between Price Index and market access from Equation (A4) that

$$P_o^{-\theta} = \rho^{-1} MA_o \tag{A11}$$

In the next step, we solve for the relationship between labor and market access. The equations (A7) and (A8) give us,

$$Y_o = \kappa_1 A_o (q_o^{\alpha} w_o^{\gamma})^{-\theta} MA_o \tag{A12}$$

Assuming mobile labor, the real wage and utility are equalized across locations. Nominal wages are given by

$$w_o = \bar{U} \times P_o \tag{A13}$$

where $\bar{U}$ is the utility level.

According to the Cobb-Douglas production function, the rental rate of land and the nominal wage of labor are related to their income share, such that

$$q_o T_o = \alpha Y_o \tag{A14}$$

$$w_o L_o = \gamma Y_o \tag{A15}$$

Using equations (A11), (A13), (A14), and (A15) in Equation (A12), solving for labor yields:[7]

$$\ln L_o = \kappa_2 + \frac{1}{1+\theta\alpha} \ln A_o + \frac{-1-\theta(\alpha+\gamma)}{1+\theta\alpha} \ln \bar{U} + \frac{\theta\alpha}{1+\theta\alpha} \ln T_o + \frac{1+\theta(1+\alpha+\gamma)}{\theta(1+\theta\alpha)} \ln MA_o \tag{A16}$$

Besides, using equation (A11), (A13), and (A15), the equation (A10) implies:[8]

$$MA_o = \kappa_3 \sum_d \tau_{od}^{-\theta} MA_d^{-(1+\theta)/\theta} L_d \tag{A17}$$

D.2 Estimating θ

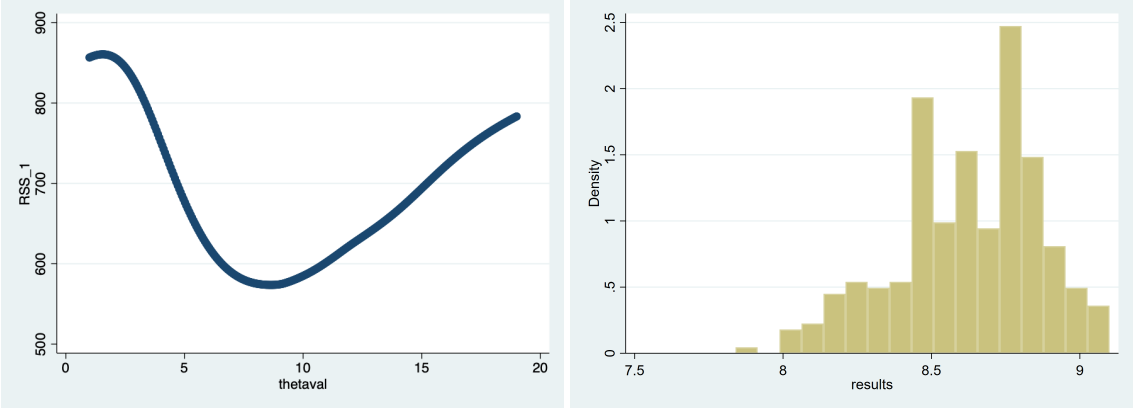
As presented in Equation (A16), in time t, we have $lnL_{ot} = f(\theta)_{ot} + \epsilon_{ot}$, where $f(\theta)_{ot} = \frac{1+\theta(1+\alpha+\gamma)}{\theta(1+\theta\alpha)} lnMA(\theta)_{ot}$. $MA(\theta)_{ot}$ is decided implicitly by Equation (A17) given the trade cost matrix τ_{od}, population L_d and θ at time t. This is a NLS problem because $f(\theta)_{ot}$ is nonlinear in the parameter θ. Besides, we assume ϵ_{ot} is orthogonal to $f(\theta)_{ot}$ conditional on a set of control on geographical and agricultural factors as described in Section 2.2. We obtain the NLS best

[7] Here, $\kappa_2 = \frac{\ln \kappa_1}{1+\theta\alpha} + \frac{\alpha\theta}{1+\theta\alpha} \ln \alpha - \ln \gamma + \frac{1+\theta(\alpha+\gamma)}{\theta(1+\theta\alpha)} \ln \rho$.

[8] Here, $\kappa_3 \equiv \frac{\bar{U}\rho^{\frac{1+\theta}{\theta}}}{\gamma}$.

fitted θ using a grid search over θ based on an evenly spaced grid with 300 points. Following the existing papers, we use $\alpha = 0.4$ and $\gamma = 0.55$ as land and labor shares to compute $f(\theta)_{ot}$ (Brandt, 1989; Perkins, 2017). As shown in Figure D.2a, the θ with least RSS value is 8.62. And its 95% confidence interval is [8.08-9.04] based on bootstrapping at the grid-level, with 300 replications (the distribution of theta values as shown in Figure D.2b) .

Figure D.2: NLS Theta Selection Plots



(a) RSS Values

Notes: Theta with least RSS is selected ($\theta = 8.62$).

(b) Distribution of NLS Selected Theta

Notes: 95% Confidence Interval is [8.08-9.04] around the estimated theta value 8.62.

D.3 Model-Derived MA vs. Simple Approximation

Table D.3 compares the impacts of model-derived and simple approximated market access on population density. When we instrument for market access and used standardize the two sets of market access measures, we obtain similar elasticities.

Table D.3: Model-Derived MA vs. Simple Approximation

Dependent variable	ln MA (std.) (1)	ln MA (model-based, std.) (2)	ln Popu. Density (3)	ln Popu. Density (4)	ln MA (std.) (5)	ln MA (model-based, std.) (6)	ln Popu. Density (7)	ln Popu. Density (8)
	First-Stage		IV: ln MA (optimal, pre-1500 CSI,std.)		First-Stage		IV: ln MA (optimal, Tang popu., std.)	
ln MA (optimal, pre-1500 CSI,std.)	0.459***	0.441***						
	(0.044)	(0.050)						
ln MA (optimal, Tang popu., std.)					0.605***	0.583***		
					(0.047)	(0.054)		
ln MA (std.)			0.363***				0.548***	
			(0.102)				(0.100)	
ln MA (model-based, std.)				0.378***				0.569***
				(0.091)				(0.082)
Grid FE	Y	Y	Y	Y	Y	Y	Y	Y
Year FE	Y	Y	Y	Y	Y	Y	Y	Y
GeoControl × Year FE	Y	Y	Y	Y	Y	Y	Y	Y
AgriControl × Dynasty FE	Y	Y	Y	Y	Y	Y	Y	Y
KP F-stat			107.39	76.82			167.08	116.36
R-squared	0.886	0.879	0.045	0.354	0.891	0.884	0.018	0.478
Observations	3,249	3,249	3,249	3,249	3,249	3,249	3,249	3,249

Notes: Columns (1)-(2) and (5)-(6) are first-stage regressions of standardized simple and model-derived ln MA on the optimal-route instrument; columns (3)-(4) and (7)-(8) report the corresponding second-stage IV estimates on population density. Control variables are the same as those listed in Table 1. Standard errors displayed in parentheses are clustered at grid level. *** $p < 0.01$, ** $p < 0.05$, * $p < 0.1$.

D.4 Counterfactual Analysis

As in Donaldson and Hornbeck (2016), the counterfactuals can be solved by either assuming $\bar{U}$ is constant across counterfactuals and the total population adjusts, or the total population is constant and $\bar{U}$ adjusts. We are interested in the impact of market access on population density in our paper, so we focus on the first case, which allows for population mobile and require utility $\bar{U}$ is constant (Specifically, we assume $\bar{U} = 1$).

Our goal is to solve for new equilibrium of population distribution and aggregated population in each dynasty assuming that the route of Grand Canal remains unchanged after Song dynasty. This counterfactual exercise depends on the changing matrix of trade cost τ_{od} in the model, while holding the productivity term A_o and the exogenous land area T_o for each grid fixed at their actual level in each dynasty. The first problem is that A_o and T_o are unobserved in our study. We therefore show the procedure to estimate the unknown terms through our model, from the available data on population and actual matrix of τ_{od} in each dynasty.

We begin with estimating the price index using the Equation (A17). With $P_o^{-\theta} = \rho^{-1} MA_o$, the Equation (A17) can be re-written as

$$P_o^{-\theta} = \sum_d \frac{\tau_{od}^{-\theta} P_d L_d}{\sum_i \tau_{di}^{-\theta} P_i^{1+\theta} L_i}. \tag{A18}$$

Given the actual population L_o of each grid and the actual matrix of trade cost τ_{od} in each period, we can first estimate the actual price index P_o for each grid in each year.

Then, substituting $w_o = \bar{U} \times P_o, q_o T_o = \alpha Y_o$, and $w_o L_o = \gamma Y_o$ into the Equation(A5) and assuming the good markets clear yields that,

$$\kappa_1 \alpha^{-\alpha\theta} A_o T_o^{\theta\alpha} = P_o^{1+\theta(\alpha+\gamma)} \times \left(\frac{L_o}{\gamma}\right)^{1+\alpha\theta} \times \left(\sum_i \tau_{oi}^{-\theta} P_i^{1+\theta} \frac{L_i}{\gamma}\right)^{-1} \times \bar{U}^{1+\theta(\alpha+\gamma)}. \tag{A19}$$

We define the unknown term as $C_o \equiv A_o T_o^{\theta\alpha}$. Holding $\bar{U} = 1$, we have,

$$C_o \kappa_1 \alpha^{-\alpha\theta} \sum_i \tau_{oi}^{-\theta} P_i^{1+\theta} \frac{L_i}{\gamma} = P_o^{1+\theta(\alpha+\gamma)} \left(\frac{L_o}{\gamma}\right)^{1+\alpha\theta}. \tag{A20}$$

Given the price index P_o estimated from Equation (A18), actual population distribution L_o and the given parameters (θ, α and γ), we can back out the unknown term C_o, which is fixed in each year in the counterfactual exercise.

Then we show the procedure for solving the counterfactual labor distribution. Following Hornbeck and Rotemberg (2024), we use the Perron-Frobenius theorem to show the uniqueness of the counterfactual solutions. The main idea of Perron-Frobenius theorem is that, for any matrix M, with all its elements positive, the equation $\hat{\phi}\lambda = M\hat{\phi}$ has a unique eigenvalue λ and a unique (up to proportionality) eigenvector $\hat{\phi}$ with all its elements positive.

With the assumption $\bar{U} = 1$, and $w_o = \bar{U} \times P_o, q_o T_o = \alpha Y_o, w_o L_o = \gamma Y_o$, Equation (A4) derives

$$(P_o)^{-\theta} = \kappa_1 \alpha^{-\alpha\theta} \sum_i C_i P_i^{-\theta(\alpha+\gamma)} \left(\frac{L_i}{\gamma}\right)^{-\alpha\theta} (\tau_{oi})^{-\theta}. \tag{A21}$$

Then we solve the equation system of Equations (A20) and (A21).

We first define a term ϕ_o,

$$\phi_o \equiv \frac{{P_o}^{-\theta} C_o \kappa_1 \alpha^{-\alpha\theta}}{P_o^{1+\theta(\alpha+\gamma)} \left(\frac{L_o}{\gamma}\right)^{1+\alpha\theta}}. \tag{A22}$$

Taking Equation (A21) into Equation (A22), we have,

$$\phi_o = \frac{(\kappa_1 \alpha^{-\alpha\theta})^2 C_o}{P_o^{1+\theta(\alpha+\gamma)} \left(\frac{L_o}{\gamma}\right)^{1+\alpha\theta}} \times \sum_i C_i P_i^{-\theta(\alpha+\gamma)} \left(\frac{L_i}{\gamma}\right)^{-\alpha\theta} (\tau_{oi})^{-\theta} \tag{A23}$$

Since $\phi_i \equiv \frac{\kappa_1 \alpha^{-\alpha\theta} {P_i}^{-\theta} C_i}{P_i^{1+\theta(\alpha+\gamma)} (\frac{L_i}{\gamma})^{1+\alpha\theta}}$, the equation (A23) can be re-written as,

$$\phi_o = \frac{\kappa_1 \alpha^{-\alpha\theta} C_o}{P_o^{1+\theta(\alpha+\gamma)} \left(\frac{L_o}{\gamma}\right)^{1+\alpha\theta}} \times \sum_i \phi_i P_i^{1+\theta} (\tau_{oi})^{-\theta} \frac{L_i}{\gamma} \tag{A24}$$

The equation (A20) can be written as,

$$1 = \frac{\kappa_1 \alpha^{-\alpha\theta} \sum_i C_o \tau_{oi}^{-\theta} P_i^{1+\theta} \frac{L_i}{\gamma}}{P_o^{1+\theta(\alpha+\gamma)} \left(\frac{L_o}{\gamma}\right)^{1+\alpha\theta}} \tag{A25}$$

We define a matrix A with elements $[A_{od}] = [\frac{\kappa_1 \alpha^{-\alpha\theta} C_o \tau_{od}^{-\theta} P_d^{1+\theta} L_d}{P_o^{1+\theta(\alpha+\gamma)} (\frac{L_o}{\gamma})^{1+\alpha\theta} \gamma}]$. All of the elements in matrix A are positive. According to the Perron-Frobenius theorem, if the equation system (A24) and (A25) holds, we have two eigenvectors $[\phi_o]$ and $[1]$ that are proportional. Therefore,$\phi_o = \phi^{-1} \times 1$, for some constant ϕ^{-1}.

Then, the equation (A22) turns into:

$$P_o^{1+\theta(1+\alpha+\gamma)} = \kappa_1 \alpha^{-\alpha\theta} C_o \left(\frac{L_o}{\gamma}\right)^{-1-\alpha\theta} \phi \tag{A26}$$

Substituting equation (A26) into equation (A20), and let $g = 1 + \theta(1 + \alpha + \gamma)$, we have:

$(\kappa_1 \alpha^{-\alpha\theta})^{\frac{2\theta+1}{g}} C_o \sum_i \tau_{oi}^{-\theta} (C_i (\frac{L_i}{\gamma})^{-1-\alpha\theta} \phi)^{\frac{\theta+1}{g}} \times \frac{L_i}{\gamma} = (C_o (\frac{L_o}{\gamma})^{-1-\alpha\theta} \phi)^{\frac{\theta(\alpha+\gamma)+1}{g}} \times (\frac{L_o}{\gamma})^{1+\theta\alpha}$

After rearranging, we have the final equation on the counterfactual population distribution as follows,

$$\phi^{\frac{\theta(1-\alpha-\gamma)}{g}} \gamma^{\left(\frac{(\theta\alpha+1)(1+2\theta)}{g}-1\right)} (\kappa_1 \alpha^{-\alpha\theta})^{\frac{2\theta+1}{g}} \times C_o^{\frac{\theta}{g}} \sum_i \tau_{oi}^{-\theta} C_i^{\frac{1+\theta}{g}} L_i^{1-\frac{(1+\theta)(1+\theta\alpha)}{g}} = L_o^{\frac{\theta(1+\theta\alpha)}{g}} \tag{A27}$$

Based on equation (A27),[9] given counterfactual matrix $[\tau_{od}]$ and unchanged term C_o,we can derive the counterfactual population distribution L_o for each grid in different periods.

[9]Following Donaldson and Hornbeck (2016), we assume $\frac{r}{f(P)} = \bar{r}$, where$\bar{r}$ is exogenous foreign real interest rate and $f(P)$ is the population-weighted price index of the goods that are implicitly traded for foreign capital. $f(P)$ is equal to $\sum_d \frac{L_d P_d}{\sum_d L_d}$ in our model. Although the interest rate r changes with price indices P_i, it is equalized across grids. So, it does not affect the counterfactual population distribution across grids.

D.5 Checks on Counterfactual Estimates: Capital vs. Canal

One concern is that the lower aggregate population implied by the Beijing–Hangzhou route, relative to the Central Plains route, may reflect the direct effect of Beijing as the political capital rather than the effect of the canal itself. In other words, the counterfactual results might be driven by changes in the productivity or attractiveness of capital locations, especially Beijing, rather than by the transportation network. To address this concern, we conduct two robustness checks that exclude capital-related grids from the analysis. First, we drop the five grids into which the coordinates of historical capitals fall (Table D.5.a). Second, we further exclude the main grids covered by each dynasty's capital prefecture, defined as grids for which the overlap area accounts for at least 20% of the grid area, resulting in 19 excluded grids in total (Table D.5.b). The counterfactual results under both sample restrictions are very similar to the baseline results, suggesting that our findings are unlikely to be driven by a direct capital effect and instead reflect the role of the canal network.

Table D.5.a: Robustness Check on Counterfactual Estimates by Dropping Capital Grids

	Popu. Changes (%)								
Year	741	980	1080	1102	1290	1393	1580	1776	1820
	(1)	(2)	(3)	(4)	(5)	(6)	(7)	(8)	(9)
A. Drop the Grand Canal									
Land Road Cost Unchanged	-5.07	-4.76	-4.89	-4.72	-5.49	-5.94	-6.08	-2.54	-2.52
Land Road Cost Decline 20%	-2.76	-2.76	-2.92	-2.78	-3.21	-3.56	-3.59	0.16	0.15
Land Road Cost Decline 30%	-1.19	-1.45	-1.64	-1.52	-1.72	-2.04	-2.00	1.89	1.87
Land Road Cost Decline 40%	0.78	0.14	-0.08	0.02	0.09	-0.21	-0.08	3.99	3.95
Land Road Cost Decline 50%	3.28	2.15	1.91	1.98	2.34	2.04	2.27	6.58	6.51
B. Adopt Grand Canal in Other Dynasty									
Adopt Grand Canal in Tang Dynasty		-1.63	-2.03	-1.94	-0.88	0.85	1.03	0.94	0.95
Adopt Grand Canal in Song Dynasty	1.41				-1.71	1.21	1.15	1.86	1.83
Adopt Grand Canal in Yuan Dynasty	-0.69	-1.39	-1.37	-1.39		0.07	0.05	0.19	0.21
Adopt Grand Canal in Ming/Qing Dynasty	-2.78	-3.88	-3.73	-3.61	-1.73				

Notes: This table reports the percentage change in aggregate population, relative to the actual population, implied by counterfactual transportation networks solved from the structural model (Appendix D.1), holding each grid's productivity and land endowment fixed at the levels backed out from the actual network and actual population in that sample year. This table replicates Table 3 after dropping the five ever-capital grids, where the centroids of capital prefectures were located.

Table D.5.b: Robustness Check on Counterfactual Estimates by Dropping Capital Related Grids

	Popu. Changes (%)								
Year	741	980	1080	1102	1290	1393	1580	1776	1820
	(1)	(2)	(3)	(4)	(5)	(6)	(7)	(8)	(9)
A. Drop the Grand Canal									
Land Road Cost Unchanged	-4.77	-4.34	-4.48	-4.32	-5.39	-5.11	-5.32	-2.43	-2.41
Land Road Cost Decline 20%	-3.02	-2.94	-3.07	-2.95	-3.27	-3.57	-3.60	0.23	0.22
Land Road Cost Decline 30%	-1.37	-1.60	-1.76	-1.65	-1.77	-2.03	-1.99	2.00	1.97
Land Road Cost Decline 40%	0.71	0.04	-0.16	-0.07	0.05	-0.17	-0.05	4.13	4.09
Land Road Cost Decline 50%	3.35	2.12	1.89	1.95	2.32	2.10	2.33	6.78	6.70
B. Adopt Grand Canal in Other Dynasty									
Adopt Grand Canal in Tang Dynasty		-1.43	-1.81	-1.72	-0.91	0.68	0.83	0.56	0.58
Adopt Grand Canal in Song Dynasty	1.05				-1.71	1.24	1.22	1.39	1.37
Adopt Grand Canal in Yuan Dynasty	-0.39	-1.06	-1.06	-1.08		0.05	0.03	0.14	0.15
Adopt Grand Canal in Ming/Qing Dynasty	-2.30	-3.43	-3.29	-3.18	-1.76				

Notes: This table reports the percentage change in aggregate population, relative to the actual population, implied by counterfactual transportation networks solved from the structural model (Appendix D.1), holding each grid's productivity and land endowment fixed at the levels backed out from the actual network and actual population in that sample year. This table replicates Table 3 under two alternative sample restrictions: first, by dropping the five ever-capital grids, where the centroids of capital prefectures were located; and second, by further dropping the main grids covered by the capital prefecture in each dynasty, defined as grids for which the overlap area accounts for at least 20% of the grid area, resulting in a total of 19 excluded grids.

D.6 Alternative Counterfactual Estimates

Table D.6.a presents the reduced-form projections, using the same cost assumption as that in our main analysis. Table D.6.b presents model-derived counterfactual under different assumptions of trade cost. Finally, Table D.6.c presents reduced-form projections under different cost assumptions.

Table D.6.a: Reduced-Form Counterfactual Estimates: Dropping and Relocating the Grand Canal

	Popu. Changes (%)								
Year	741	980	1080	1102	1290	1393	1580	1776	1820
	(1)	(2)	(3)	(4)	(5)	(6)	(7)	(8)	(9)
A. Drop the Grand Canal									
Land Road Cost Unchanged	-9.26	-6.23	-6.42	-6.33	-7.74	-8.54	-8.47	-3.40	-3.38
	(1.07)	(0.74)	(0.76)	(0.75)	(0.92)	(1.00)	(0.99)	(0.41)	(0.40)
Land Road Cost Decline 20%	-5.51	-3.27	-3.63	-3.53	-4.25	-5.48	-5.36	0.00	-0.02
	(0.63)	(0.39)	(0.43)	(0.42)	(0.51)	(0.64)	(0.62)	(0.01)	(0.01)
Land Road Cost Decline 30%	-3.27	-1.55	-2.00	-1.89	-2.22	-3.70	-3.54	1.98	1.93
	(0.35)	(0.18)	(0.23)	(0.22)	(0.26)	(0.42)	(0.40)	(0.27)	(0.26)
Land Road Cost Decline 40%	-0.69	0.38	-0.16	-0.05	0.06	-1.71	-1.51	4.19	4.12
	(0.03)	(0.07)	(0.00)	(0.01)	(0.02)	(0.18)	(0.15)	(0.56)	(0.55)
Land Road Cost Decline 50%	2.29	2.63	2.00	2.11	2.65	0.55	0.79	6.71	6.61
	(0.35)	(0.36)	(0.28)	(0.29)	(0.36)	(0.11)	(0.15)	(0.90)	(0.88)
B. Adopt Grand Canal in Other Dynasty									
Adopt Grand Canal in Tang Dynasty		-1.95	-2.61	-2.55	-1.47	0.89	1.10	1.37	1.41
		(0.23)	(0.31)	(0.30)	(0.18)	(0.12)	(0.15)	(0.19)	(0.20)
Adopt Grand Canal in Song Dynasty	2.38				-2.59	1.11	0.97	2.37	2.31
	(0.34)				(0.32)	(0.15)	(0.13)	(0.32)	(0.31)
Adopt Grand Canal in Yuan Dynasty	-1.48	-2.02	-1.99	-2.06		0.11	0.06	0.28	0.31
	(0.16)	(0.24)	(0.23)	(0.24)		(0.01)	(0.01)	(0.04)	(0.04)
Adopt Grand Canal in Ming/Qing Dynasty	-5.36	-5.11	-4.88	-4.83	-6.03				
	(0.62)	(0.61)	(0.58)	(0.57)	(0.59)				

Notes: This table reports the percentage change in aggregate population, relative to actual levels, based on the reduced-form estimates (Table 2, column (2)). The implied population change for each grid is calculated from the change in market access and the estimated elasticity of population density with respect to market access (population density fall by 0.143 logs for 1-log decline in market access). All grids in each sample year are included in the counterfactual estimates. Standard errors are reported in parentheses, clustered at the grid level.

Table D.6.b: Model-based Counterfactual Estimates (Different Assumptions)

	Popu. Changes (%)								
Year	741	980	1080	1102	1290	1393	1580	1776	1820
	(1)	(2)	(3)	(4)	(5)	(6)	(7)	(8)	(9)
A. Drop the Grand Canal									
Alt. Route Cost (Assump. 1)	-7.13	-6.81	-6.93	-6.75	-7.34	-8.15	-8.45	-3.82	-3.80
Alt. Route Cost (Assump. 2)	-5.21	-4.61	-4.69	-4.55	-5.23	-5.59	-5.70	-2.31	-2.29
Alt. Route Cost (Assump. 3)	-7.15	-7.06	-7.19	-6.99	-7.51	-8.21	-8.50	-3.79	-3.77
Alt. Route Cost (Assump. 4)	-5.36	-4.84	-4.95	-4.81	-5.35	-5.78	-5.88	-2.36	-2.35
Alt. Route Cost (Assump. 5)	-5.53	-5.37	-5.43	-5.27	-5.91	-6.70	-6.85	-2.84	-2.83
B.1. Adopt Tang Dynasty Grand Canal									
Alt. Route Cost (Assump. 1)		-1.67	-2.36	-2.29	-1.36	1.14	1.46	1.83	1.89
Alt. Route Cost (Assump. 2)		-0.76	-1.15	-1.08	0.16	1.85	2.13	2.26	2.29
Alt. Route Cost (Assump. 3)		-1.84	-2.52	-2.44	-1.19	1.42	1.83	2.15	2.22
Alt. Route Cost (Assump. 4)		-0.89	-1.29	-1.21	0.23	2.06	2.43	2.42	2.46
Alt. Route Cost (Assump. 5)		-1.66	-2.11	-2.03	-0.84	1.38	1.73	1.42	1.47
B.2. Adopt Song Dynasty Grand Canal									
Alt. Route Cost (Assump. 1)	1.94				-2.80	1.96	1.85	3.33	3.28
Alt. Route Cost (Assump. 2)	1.31				-1.64	1.20	1.16	1.99	1.95
Alt. Route Cost (Assump. 3)	1.68				-2.63	1.90	1.81	3.33	3.28
Alt. Route Cost (Assump. 4)	1.29				-1.50	1.22	1.21	2.06	2.02
Alt. Route Cost (Assump. 5)	1.23				-1.93	1.40	1.38	2.19	2.15
B.3. Adopt Yuan Dynasty Grand Canal									
Alt. Route Cost (Assump. 1)	-1.21	-1.88	-1.77	-1.84		0.06	0.05	0.66	0.69
Alt. Route Cost (Assump. 2)	0.11	-0.73	-0.67	-0.70		0.98	1.00	1.25	1.26
Alt. Route Cost (Assump. 3)	-1.56	-2.08	-1.99	-2.05		0.08	0.07	0.56	0.60
Alt. Route Cost (Assump. 4)	-0.23	-0.93	-0.90	-0.93		0.94	0.95	1.10	1.11
Alt. Route Cost (Assump. 5)	-1.42	-1.76	-1.66	-1.70		0.06	0.03	0.17	0.20
B.4. Adopt Ming/Qing Dynasty Grand Canal									
Alt. Route Cost (Assump. 1)	-3.65	-5.36	-4.99	-4.88	-2.84				
Alt. Route Cost (Assump. 2)	-3.15	-3.87	-3.66	-3.57	-0.66				
Alt. Route Cost (Assump. 3)	-3.88	-5.66	-5.34	-5.23	-2.68				
Alt. Route Cost (Assump. 4)	-3.29	-4.04	-3.89	-3.80	-0.61				
Alt. Route Cost (Assump. 5)	-3.23	-4.38	-4.14	-4.04	-1.96				

Notes: This table reports the aggregate effects of counterfactual networks under alternative cost assumptions, derived from the structural model. The estimated parameter θ (via NLS) for alternative route costs across Assumptions 1–5 is 8.2, 9.4, 7.3, 8.14, and 5.68, respectively. Assumptions 1–5 are listed in Appendix Table A.2.

Table D.6.c: Reduced-Form Counterfactual Estimates (Different Assumptions)

	Popu. Changes (%)								
Year	741	980	1080	1102	1290	1393	1580	1776	1820
	(1)	(2)	(3)	(4)	(5)	(6)	(7)	(8)	(9)
A. Drop the Grand Canal									
Alt. Route Cost (Assump. 1)	-15.39	-11.60	-11.75	-11.58	-13.85	-14.65	-14.83	-6.73	-6.70
	(1.46)	(1.13)	(1.14)	(1.13)	(1.35)	(1.40)	(1.42)	(0.66)	(0.66)
Alt. Route Cost (Assump. 2)	-9.70	-6.47	-6.67	-6.58	-8.24	-9.06	-8.99	-3.53	-3.52
	(1.06)	(0.73)	(0.75)	(0.74)	(0.93)	(1.00)	(0.99)	(0.40)	(0.40)
Alt. Route Cost (Assump. 3)	-12.75	-9.27	-9.43	-9.30	-11.02	-11.68	-11.73	-5.25	-5.23
	(1.39)	(1.04)	(1.05)	(1.04)	(1.24)	(1.29)	(1.29)	(0.59)	(0.59)
Alt. Route Cost (Assump. 4)	-7.60	-4.97	-5.17	-5.10	-6.10	-6.93	-6.82	-2.62	-2.62
	(0.95)	(0.64)	(0.66)	(0.65)	(0.79)	(0.88)	(0.87)	(0.34)	(0.34)
Alt. Route Cost (Assump. 5)	-9.71	-6.48	-6.67	-6.58	-8.08	-9.08	-8.97	-3.58	-3.57
	(1.13)	(0.78)	(0.80)	(0.78)	(0.97)	(1.07)	(1.05)	(0.43)	(0.43)
B.1. Adopt Tang Dynasty Grand Canal									
Alt. Route Cost (Assump. 1)		-2.92	-4.20	-4.10	-3.01	1.47	1.76	3.12	3.20
		(0.27)	(0.41)	(0.40)	(0.31)	(0.17)	(0.21)	(0.43)	(0.44)
Alt. Route Cost (Assump. 2)		-0.94	-1.66	-1.58	-0.14	2.07	2.29	2.76	2.79
		(0.10)	(0.18)	(0.17)	(0.01)	(0.26)	(0.29)	(0.36)	(0.36)
Alt. Route Cost (Assump. 3)		-2.43	-3.40	-3.32	-2.23	1.19	1.44	2.35	2.42
		(0.26)	(0.38)	(0.37)	(0.26)	(0.15)	(0.19)	(0.34)	(0.34)
Alt. Route Cost (Assump. 4)		-0.87	-1.42	-1.36	-0.14	1.49	1.67	1.90	1.93
		(0.10)	(0.18)	(0.17)	(0.02)	(0.21)	(0.23)	(0.27)	(0.28)
Alt. Route Cost (Assump. 5)		-1.97	-2.67	-2.60	-1.58	0.98	1.21	1.42	1.47
		(0.23)	(0.32)	(0.31)	(0.19)	(0.13)	(0.17)	(0.21)	(0.21)
B.2. Adopt Song Dynasty Grand Canal									
Alt. Route Cost (Assump. 1)	3.94				-5.58	2.54	2.16	5.54	5.44
	(0.53)				(0.57)	(0.31)	(0.27)	(0.71)	(0.70)
Alt. Route Cost (Assump. 2)	2.60				-2.83	1.24	1.08	2.53	2.47
	(0.35)				(0.33)	(0.16)	(0.14)	(0.33)	(0.32)
Alt. Route Cost (Assump. 3)	2.85				-4.07	1.73	1.45	3.88	3.80
	(0.41)				(0.47)	(0.23)	(0.20)	(0.53)	(0.52)
Alt. Route Cost (Assump. 4)	2.04				-1.89	0.86	0.77	1.77	1.72
	(0.31)				(0.25)	(0.12)	(0.11)	(0.25)	(0.25)
Alt. Route Cost (Assump. 5)	2.47				-2.81	1.17	1.03	2.45	2.39
	(0.36)				(0.35)	(0.16)	(0.14)	(0.34)	(0.33)
B.3. Adopt Yuan Dynasty Grand Canal									
Alt. Route Cost (Assump. 1)	-2.49	-3.30	-3.10	-3.22		0.08	0.04	1.18	1.25
	(0.20)	(0.31)	(0.29)	(0.30)		(0.01)	(0.01)	(0.15)	(0.16)
Alt. Route Cost (Assump. 2)	0.15	-0.93	-0.95	-1.02		1.25	1.20	1.69	1.71
	(0.04)	(0.10)	(0.10)	(0.11)		(0.15)	(0.15)	(0.21)	(0.21)
Alt. Route Cost (Assump. 3)	-2.27	-2.72	-2.63	-2.72		0.10	0.05	0.73	0.78
	(0.24)	(0.30)	(0.29)	(0.30)		(0.01)	(0.01)	(0.10)	(0.10)
Alt. Route Cost (Assump. 4)	-0.18	-0.92	-0.97	-1.02		0.83	0.78	1.04	1.05
	(0.01)	(0.11)	(0.12)	(0.13)		(0.11)	(0.11)	(0.14)	(0.15)
Alt. Route Cost (Assump. 5)	-1.70	-2.11	-2.05	-2.12		0.13	0.07	0.30	0.33
	(0.19)	(0.25)	(0.24)	(0.25)		(0.02)	(0.01)	(0.04)	(0.05)
B.4. Adopt Ming Dynasty Grand Canal									
Alt. Route Cost (Assump. 1)	-8.36	-9.21	-8.47	-8.35	-5.56				
	(0.77)	(0.90)	(0.82)	(0.80)	(0.57)				
Alt. Route Cost (Assump. 2)	-5.72	-5.37	-5.10	-5.04	-1.27				
	(0.62)	(0.60)	(0.57)	(0.56)	(0.14)				
Alt. Route Cost (Assump. 3)	-7.12	-7.44	-6.97	-6.89	-4.08				
	(0.77)	(0.84)	(0.78)	(0.77)	(0.48)				
Alt. Route Cost (Assump. 4)	-4.38	-4.07	-3.95	-3.92	-0.90				
	(0.55)	(0.53)	(0.51)	(0.50)	(0.12)				
Alt. Route Cost (Assump. 5)	-5.62	-5.29	-5.02	-4.98	-2.83				
	(0.65)	(0.64)	(0.60)	(0.59)	(0.35)				

Notes: This table reports the aggregate effects of counterfactual networks under alternative cost assumptions, based on reduced-form estimates. Standard errors are reported in parentheses, clustered at the grid level. The estimated parameter θ (via NLS) for alternative route costs across Assumptions 1–5 is 8.2, 9.4, 7.3, 8.14, and 5.68, respectively. Assumptions 1–5 are listed in Appendix Table A.2.